RIGA TECHNICAL UNIVERSITY

Artūrs ABOLTINS

SYNCHRONIZATION AND EQUALIZATION FOR MULTICARRIER SYSTEMS WITH PARAMETRIC GENERALIZED UNITARY ROTATION BASED MODULATION

Summary of doctoral thesis

Riga 2013

RIGA TECHNICAL UNIVERSITY

Faculty of Electronics and Telecommunications

Institute of Radio Electronics

Arturs ABOLTINS

Student of the Doctoral study program “Electronics”

SYNCHRONIZATION AND EQUALIZATION FOR MULTICARRIER SYSTEMS WITH PARAMETRIC GENERALIZED UNITARY ROTATION BASED MODULATION

Summary of doctoral thesis

Academic supervisor

Dr. sc. ing., professor

P. MISANS

RTU Press

Riga 2013

UDK 621.396.21(043.2)
Ab 668 s

Aboltins A. Synchronization and equalization for multicarrier systems with parametric generalized unitary rotation based modulation. Summary of doctoral thesis. R.:RTU Press, 2013. -45 p.

Printed according to the decision of FET promotion council “RTU P-08” on June 27, 2013, protocol No. 16.

EIROPAS SAVIENĪBA

ESF
EIROPAS SOCIĀLAIS FONDS

This work has been supported by the European Social Fund within the project “Support for the implementation of doctoral studies at Riga Technical University”.

ISBN 978-9934-10-461-9

A DOCTORAL THESIS SUBMITTED TO RIGA TECHNICAL UNIVERSITY IN FULFILLMENT OF THE REQUIREMENTS FOR THE DEGREE OF DOCTOR OF SCIENCE IN ENGINEERING

The public defense of the doctoral thesis for promotion to the doctor's degree in engineering will take place on 10th of October, 2013, at 17:45 in Room 102, Faculty of Electronics and Telecommunications, Azenes 12.

OFFICIAL REVIEWERS

Professor, Dr.sc.ing. Guntars Balodis
Faculty of Electronics and Telecommunications, Riga Technical University, Latvia

Professor, Dr.habil.ing. Andreas Ahrens
Hochschule Wismar, University of Applied Sciences Technology, Business and Design, Faculty of Engineering, Department of Electrical Engineering and Computer Science, Germany

Senior Researcher Dr.habil.math. Aivars Lorencs
Institute of Electronics and Computer Science, Latvia

CONFIRMATION

I confirm that this doctoral thesis, submitted for a degree in engineering at the Riga Technical University, is my own work. The doctoral thesis has not been submitted for a degree in any other university.

Arturs Aboltins .... (Signature)

Date: ....

The doctoral thesis is written in English, contains introduction, 8 chapters, conclusions, references, 2 appendices, index, 70 Figures and 9 Tables, 156 pages in total. The list of references consists of 107 titles.

Contents

1 General description of the work **7**
- 1.1 Urgency of the subject matter . . . 7
- 1.2 Objective of the work . . . 8
- 1.3 Scientific novelty and main results . . . 8
- 1.4 Theses to be defended . . . 9
- 1.5 Research technique . . . 9
- 1.6 Research object . . . 10
- 1.7 Practical significance of the research . . . 10
- 1.8 Approbation . . . 11

2 Baseband components **12**
- 2.1 Structure of a parametric multicarrier modulation system . . . 12
- 2.2 Structure of baseband signals . . . 14
- 2.3 Synchronization sequences . . . 16
- 2.4 Transmit filtering and upconversion . . . 17

3 Multicarrier modulation **18**
- 3.1 Unitary transforms for digital modulation . . . 18
- 3.2 Configurations of multicarrier modulator and demodulator . . . 19
- 3.3 Peak-to-average power ratio of the multicarrier signal . . . 21
- 3.4 Transform selection for the parametric multicarrier modulation system . . . 22

4 Timing offset synchronization **23**
- 4.1 Overview . . . 23
- 4.2 Block synchronization . . . 24
- 4.3 Frame synchronization . . . 28

5 Frequency synchronization **28**
- 5.1 Types of frequency offset . . . 28
- 5.2 Impact of frequency offset . . . 29
- 5.3 Carrier frequency offset estimation . . . 30
- 5.4 Residual phase offset estimation . . . 33
- 5.5 Carrier frequency offset and phase correction . . . 33
- 5.6 FCFO synchronizer in GUR-based PMC system . . . 34

6 Channel estimation and equalization **34**
- 6.1 Introduction . . . 34
- 6.2 System model . . . 34
- 6.3 Disturbances caused by the communication channel . . . 35
- 6.4 Channel estimation . . . 35
- 6.5 Channel equalization . . . 37
- 6.6 Simulation results of equalization . . . 38
- 6.7 Comparison of channel estimation and equalization methods . . . 38

7 Design of parametric multicarrier modulation system **39**
- 7.1 Structure of the parametric multicarrier modulation system . . . 39
- 7.2 Simulation results of the model . . . 41

8 Utilization of the obtained results for future research **42**

List of abbreviations

AC autocorrelation.
ADC analog-to-digital converter.
AWGN additive white Gaussian noise.

BER bit error ratio.
BF basis function.
BTO block timing offset.

CAZAC constant amplitude zero autocorrelation.
CCDF complementary cumulative distribution function.
CCRAOT complex constant rotation angle OT.
CDMA code division multiple access.
CFO carrier frequency offset.
CP cyclic prefix.
CPU central processing unit.
CRAIMOT Constant Rotation Angle Inside Matrix OT.
CRAOT constant rotation angle OT.
CSI channel state information.

DA data-aided.
DAC digital-to-analog converter.
DD data-directed.
DFE decision-feedback equalizer.
DFT discrete Fourier transform.
DPSK differential phase shift keying.
DQAM differential quadrature amplitude modulation.
DSL digital subscriber line.
DSP digital signal processor.

EGUR Elementary Generalized Unitary Rotation.

FBMC filter bank multicarrier.
FCFO fractional carrier frequency offset.
FD frequency domain.
FDE frequency domain equalizer.
FIR finite impulse response.
FMT filtered multitone.
FPGA field-programmable gate array.
FrFT fractional Fourier transform.

GD GUR domain.
GI guard interval.
GUR Generalized Unitary Rotation.

IBI inter-block interference.
IC integrated circuit.
ICI inter-carrier interference.
IDFT inverse discrete Fourier transform.
IF intermediate frequency.
IP intellectual property.
IQ in-phase quadrature.
ISI inter-symbol interference.

LMS least mean squares.
LS least squares.

MC multicarrier.
MF matched filter.
MIMO multiple-input multiple-output.
ML maximum likelihood.
MLS maximum length sequence.
MSE mean squared error.

NCO numerically controlled oscillator.
NDA non data-aided.

OFDM orthogonal frequency division multiplexing.
OSI Open System Interconnection.
OT orthogonal transform.

P/S parallel-to-serial.
PAPR peak-to-average power ratio.
PID proportional integral derivative.
PN pseudo-noise.
PSAM pilot signal assisted modulation.

QAM quadrature amplitude modulation.

RABOT Rotation Angle Based OT.
RF radio frequency.
RLS recursive least squares.
RRC root-raised-cosine.

S/P serial to parallel.
SC single carrier.
SDR software-defined radio.
SFO sampling frequency offset.
SI super-imposed.
SINR signal-to-interference ratio.
SIS super-imposed sequence.
SNR signal-to-noise ratio.
SOGRM stairs-like orthogonal generalized rotation matrix.
SS spread spectrum.
SVD singular value decomposition.

TD time domain.

UW unique word.

WGN white Gaussian noise.
WHT Walsh-Hadamard transform.

XC cross-correlation.

ZC Zadoff-Chu.
ZP zero padding.

$\boldsymbol{X}$	transform domain samples in transmitter
$\boldsymbol{x}$	transmitted time domain (TD) baseband samples
$\boldsymbol{s}$	transmitted time domain (TD) passband samples
$\boldsymbol{x_{cp}}$	transmitted time domain (TD) baseband samples with cyclic prefix (CP)
$\boldsymbol{x_{zp}}$	transmitted time domain (TD) baseband samples with zero padding (ZP)
$\boldsymbol{x_{uw}}$	transmitted time domain (TD) baseband samples with unique word (UW) prefix
$\boldsymbol{r}$	received time domain (TD) passband samples
$\boldsymbol{Y}$	received transform domain baseband samples
$\boldsymbol{y}$	received time domain (TD) baseband samples
L	length of padding
φ	basis function
$\boldsymbol{h}$	time domain impulse response
$\boldsymbol{\Lambda}$	frequency response
$\mathit{\Lambda}$	log-likelihood function
$\boldsymbol{u}$	synchronization unique word (UW) sequence
σ	standard deviation, square root of variance
ϵ	absolute carrier frequency offset (CFO)
ε	fractional carrier frequency offset (FCFO)
$\boldsymbol{w}$	white Gaussian noise (WGN)
τ	chip time
t	time
n	transform domain index
k	time domain index
j	imaginary unit $j^2 = -1$
ϕ, γ, ψ	real-valued angle
$\boldsymbol{\Phi}$	unitary transformation matrix
$\boldsymbol{H}$	time domain (TD) channel matrix
$\hat{\boldsymbol{H}}$	estimate of time domain (TD) channel matrix
$\boldsymbol{A}$	transform domain channel matrix
$\boldsymbol{A}^{-1}$	inverse of transform domain channel matrix
$\hat{\boldsymbol{A}}$	estimate of transform domain channel matrix
$\boldsymbol{I}$	identity matrix
$\boldsymbol{B_p}$	stairs-like orthogonal generalized rotation matrix (SOGRM)
$\boldsymbol{F}$	discrete Fourier transform (DFT) matrix

Table 1: List of main mathematical symbols used in this work

$\overline{\boldsymbol{z}}$	mean of vector $\boldsymbol{z}$
$\|\|\boldsymbol{x}\|\|$	ℓ^2 norm of the vector $\boldsymbol{x}$
$\|x\|$	modulus of variable x
$\angle(x)$	angle of complex variable x
$\Re(x)$	real part of variable x
$\Im(x)$	imaginary part of variable x
$\boldsymbol{M}^*$	transposed conjugate (Hermitian adjoint) of a matrix $\boldsymbol{M}$
$\boldsymbol{M}^{-1}$	inverse of a matrix $\boldsymbol{M}$
$\langle \boldsymbol{x}, \boldsymbol{y} \rangle$	inner product between vectors $\boldsymbol{x}$ and $\boldsymbol{y}$
$\otimes$	Kronecker product
$*$	convolution
$\circledast$	circular convolution

Table 2: Mathematical notation

1 General description of the work

1.1 Urgency of the subject matter

At the beginning of 21-th century we are witnessing a rapid growth of demand for high-speed data communications. Due to the limited frequency resources and the growing geographical density of the devices, more and more efficient, low power and secure modulation techniques are required. Multicarrier (MC) communications are one of the most attractive technologies for providing high speed digital transmission. Multiple subcarriers provide an additional dimension for the mitigation of distortions caused by the propagation media and multiple access interference.

MC systems with sinusoidal basis functions (BFs), such as orthogonal frequency division multiplexing (OFDM) [1], are the most widely used MC technologies. OFDM technology became popular just a few decades ago due to the achievements in digital signal processor (DSP) hardware design [2]. It has become the modulation technique of choice in many widely-used telecommunication standards due to high spectral efficiency, achieved by means of computationally simple and powerful frequency domain (FD) equalization technique. Many modern facilities like wireless computer networks, digital television and digital subscriber line modems are based on OFDM. This modulation technique provides improved (compared to single carrier (SC) systems) spectral efficiency and ease of equalization.

Along with many advantages, the OFDM-based modulation has several serious drawbacks:

- Reduction of communication system capacity and power efficiency due to the use of cyclic prefix (CP), which is necessary for elimination of inter-block interference (IBI) and for FD equalization;
- Large envelope fluctuations, i.e. the peak-to-average power ratio (PAPR) of the time domain (TD) signal requires radio frequency (RF) power amplifiers with high dynamic range;
- High sensitivity to timing and frequency synchronization errors due to large sidelobes of individual subcarriers;
- Susceptibility to the single frequency fading/jamming because each subcarrier occupies just a small portion of the frequency spectrum.

Attempts to eliminate the mentioned drawbacks have led to several MC communication system research directions:

- Filter bank multicarrier (FBMC) communication systems. Filter banks [3], [4] utilize advanced waveforms, for instance wavelets, for obtaining higher spectral density and reduced inter-carrier interference (ICI). Good frequency localization of the mentioned systems makes them an attractive choice for cognitive radio. Problems of synchronization and equalization in these communication systems have been reviewed multiple times [5], [6]. Moreover, due to good time and frequency localization of individual subcarriers, FBMC-based systems are much more immune to synchronization errors than OFDM. However, the complexity of equalization and a large PAPR are the main show stoppers for a widespread adaptation of the mentioned modulation scheme.
- Utilization of non-sinusoidal subcarriers in order to improve immunity to the single frequency fading and narrowband jamming. In publication [7] it is shown that under certain conditions the Walsh-Hadamard transform (WHT) can outperform the discrete Fourier transform (DFT). Patent [8] describes equalization techniques for a WHT-based MC communication system. However, there are no known papers devoted to the timing and frequency synchronization in this kind of communication systems.
- Doctoral thesis [9] has provided very important results about eigenfunctions of non-stationary propagation environments. The fact that eigenfunctions of these environments are non-sinusoidal leads to ideas about the construction of more efficient modulation schemes than OFDM. Paper [10] proposes fractional Fourier transform (FrFT)-based modulation in order to improve OFDM in case of double-dispersive (time and frequency varying) communication channels. However, a much more complex decision-feedback equalizer (DFE)-based equalizer must be used in this case. Nothing on the part of timing and frequency synchronization is reviewed in [10].
- In paper [11] and in some other papers (see references in [12]) an alternative and very simple approach to performance improvement of an MC communication system, based on the transforms, which are described by a set of *rotation angles* , is proposed. It is shown that in non-Gaussian channels, the

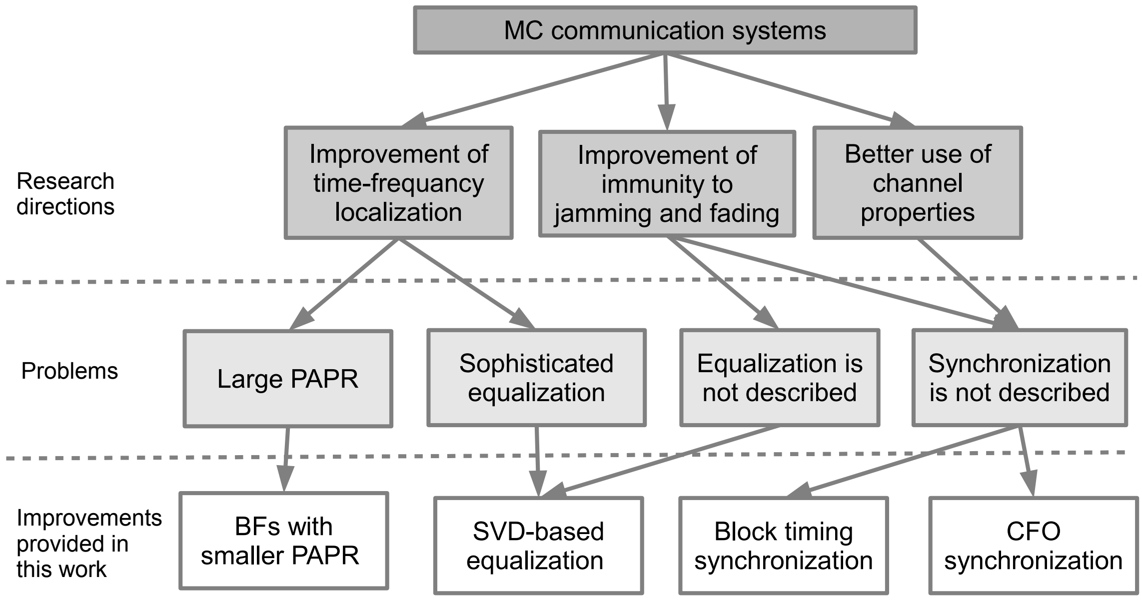

Figure 1.1: Development directions and improvements provided by this doctoral thesis

proposed communication system achieves a lower bit error ratio (BER) than the classic OFDM. The initial paper on Generalized Unitary Rotation (GUR)-based MC modulation [12] has also confirmed the possibility to use parametric unitary transformations for MC communication systems. However, no equalization and synchronization problems are discussed in these papers.

- Various hybrid schemes using spread spectrum (SS) concepts and OFDM, for instance [13], allow to improve the performance of MC communication systems. Synchronization and channel estimation in SS and code division multiple access (CDMA) communication systems have been addressed many times. However, no parametric *spreading codes* are considered in these communication systems.

This doctoral thesis is addressed to improve existing MC systems, by introduction of GUR-based parametric multicarrier (PMC) modulation, which allows to create communication systems with dynamically adjustable subcarrier waveforms. The summary of the MC communication system development directions and improvements, provided by this doctoral thesis, is given in Figure 1.1.

1.2 Objective of the work

The purpose of this work is to explore baseband algorithms of an PMC system[1], where subcarriers are produced by means of GUR. Therefore, the work has to provide a theoretical basis for the implementation of GUR-based PMC systems.

To achieve the goal, the following objectives have to be fulfilled:

- Explore GUR-based MC modulation;
- Explore timing synchronization;
- Explore frequency synchronization;
- Explore GUR domain (GD) equalization of the communication channel. A new GD equalization algorithm has to be developed.

The compatibility of the existing synchronization algorithms for other MC modulations, like OFDM, with GUR-based PMC systems has to be verified. New algorithms, if necessary, must be developed. Additionally, the impact of the accuracy of synchronization and equalization on the performance of the PMC system has to be evaluated.

1.3 Scientific novelty and main results

The following list outlines the major contributions, that have been done during writing of this doctoral thesis:

[1] description of PMC is given in Section 3.4.1

- For the first time a concept of GUR-based PMC systems is presented (Section 3.4.1).
- For the first time a method of GD equalization has been developed (Section 6.5.3.1).
- For the first time a method of GD channel estimation has been proposed (Section 6.4.2).
- For the first time a method of application of TD channel estimate to the GD has been developed (Section 6.4.1.2).
- For the first time a real-valued Rotation Angle Based OT (RABOT) rotation algorithm for the creation of the transform with a desired first BF with length $N = \mathbb{Z}$ has been developed.
- An improved method for block timing offset (BTO) estimation, based on the combination of decision-directed (DD) and data-aided (DA) estimators, has been proposed (Section 4.2.2.2).
- Several *new methods* for fractional carrier frequency offset (FCFO) estimation have been proposed (Section 5.3.2).
- Two different TD signal structures, based on the unique word (UW) prefix and super-imposed (SI) sequence, have been proposed (Sections 2.2.4.3 and 2.3.1.2).
- New configurations of unitary transformation unit - transmultiplexer and subband coder have been explored (Section 3.2.5).
- A large number of models for the simulation of communication systems and their counterparts have been created. These models can be used for teaching.

1.4 Theses to be defended

1. Using GUR it is possible to create practically usable multicarrier systems with parametric modulation.
2. Multicarrier system with parametric GUR-based modulation reduces the bit error ratio (BER) as compared to orthogonal frequency division multiplexing (OFDM) with frequency domain equalizer having the same number of subcarriers and training symbols.
3. Singular value decomposition (SVD)-based GUR domain equalizer completely mitigates inter-carrier interference, caused by the convolution in the communication channel and transmitter/receiver filters.
4. For the block timing synchronization in the multicarrier systems with parametric modulation, an estimator, which is based on the combination of proposed decision-directed cross-correlation algorithms and classic data-aided autocorrelation algorithms, must be used.
5. New, decision-directed cross-correlation based fractional carrier frequency offset (FCFO) estimation algorithms, proposed in the work, provide a maximum FCFO acquisition range, which is larger or equal to the range of classic, data-aided autocorrelation based methods.

1.5 Research technique

This research is based on the adoption of existing synchronization and channel estimation techniques for MC communication systems to GUR-based PMC systems. However, since various equalization and synchronization problems are highly related to each other, research must be done in several directions simultaneously. One of the largest challenges in this research is finding global solutions that are acceptable at all levels of communication system operation.[2]

Research included the use of both analytical and numerical approach. Most of the estimator algorithms (see, for example, Section 5.3.2) and their parameters are derived analytically. It allows to make general conclusions about the derived algorithms. However, inclusion of these algorithms into more complex systems, like synchronization loops (see, for example, Section 5.5) leads to a very complex analytical description. In these situations the numerical approach is preferred. Moreover, the numerical approach allows to verify designs in real conditions, i.e. in software where they are intended to be used.

Development of all algorithms was carried out in several steps:

- Scientific literature was explored and most suitable for the new communication system existing solutions were theoretically understood and compared to others.

[2]Synchronization and equalization are hot research topics due to the large demand for high-speed data communication solutions. The high commercial value of new synchronization and equalization algorithms leads to patenting of new inventions prior to any publications. Very frequently new algorithms do not get published at all due to intellectual property (IP) rights held by communication chip vendors.

- Potentially suitable algorithms were implemented as computer simulation scenarios. This crucial step provides a stable basis for experimentation and further research.
- Drawbacks and incompatibilities of the existing algorithms with GUR-based PMC system were figured out.
- Existing algorithms were improved or new algorithms developed.
- New approaches were verified by modification of existing model scenarios.
- Most successful findings were implemented into simplified models of the communication systems. These models were focused on a specific problem, leaving the rest of the communication system at the basic level.
- Finally, achieved results were verified using a complete PMC system model in conjunction with other already developed methods. This step checked the compatibility of the developed algorithms, and the needs for modification of the previously developed methods could be outlined.

1.6 Research object

The research object of this doctoral thesis is the *baseband* of a PMC system, where transmission is carried out using many mutually orthogonal waveforms, created using GUR. Unlike traditional MC communication systems, where the set of subcarriers is fixed, in the explored PMC systems the set of waveforms can be adjusted dynamically.

The major tasks of the researched PMC system baseband are:

- MC modulation and demodulation;
- equalization;
- timing offset synchronization;
- frequency offset synchronization.

The PMC system baseband includes the following items, which can be divided into smaller parts responsible for various specific functions:

- transmitter baseband;
- baseband equivalent of communication channel;
- receiver baseband.

The most important components of the *transmitter* baseband are:

- MC modulator;
- synchronization and training signal generator;
- pulse shaping filter.

The most important components of the *receiver* baseband are:

- timing offset synchronizer;
- FCFO synchronizer;
- communication channel equalizer;
- MC demodulator.

1.7 Practical significance of the research

Implementation of any digital data communication system is not possible without synchronization and equalization. Therefore, this doctoral thesis is oriented on solving of issues related to the practical implementation of MC systems with GUR-based modulation. At the moment of preparation of this text (June, 2013) no working prototypes of GUR-based PMC systems are available yet. However, this work can be used as an ultimate guide for building such systems.

The results of this work can be used as a general guide for building and improving non-GUR-based MC communication systems. This work contains more than 30 block diagrams and several algorithm descriptions, which allow to start practical implementation of the described devices.

The largest practical contribution of this doctoral thesis is a complete ©Mathworks Simulink model of GUR-based PMC system baseband. Moreover, dozens of different models of communication systems and separate counterparts have been created during the preparation of this work. All these models will be used for teaching students and will provide a substantial support for future research (see Chapter 8).

Reference	International	Web of science	Scopus	IEEExplore
[20]	X			
[14]	X	X		
[21]	X	X	X	
[15]	X	X	X	
[16]	X	X	X	
[17]	X	X	X	X
[18]	X	X	X	X
[19]	X	X	X	X
total	8	7	6	3

Table 1.1: References of my publications, related to this work, in databases

1.8 Approbation

The following papers have been presented in scientific conferences:

[14] Misans P., Aboltins A., Terauds M., Valters G. MATLAB/SIMULINK Implementation of Phi Transforms – A New Toolbox Only or the Rival of Wavelet Toolbox for the Next Decade? // Nordic MATLAB User Conference 2008, Stockholm, Sweden, November 20-21, 2008, pp.1-8.

[15] Aboltins A. Comparison of Orthogonal Transforms for OFDM Communication System//15th International Conference of ELECTRONICS, Kaunas, Lithuania, May 17-19, 2011.

[16] Aboltins A., Misans P., Singular Value Decomposition Based Phi Domain Equalization For Multi-Carrier Communication System // 16th International Conference of ELECTRONICS, Kaunas, Lithuania, June 18-20, 2012.

[17] Aboltins A. Block Synchronization Using a UniqueWord for a Generalized Unitary Rotation Based Communication System // 13th Biennial Baltic Electronics Conference (BEC 2012), Tallinn, Estonia, October 4-5, 2012, pp 149-152.

[18] Aboltins, A. Carrier Frequency Offset Estimator Based on Unique Word Cross-Correlation. // 20th Telecommunications Forum (TELFOR 2012) , Belgrade, Serbia, November 20-22, 2012, pp.486-489.

[19] Aboltins, A., Misans, P. Removal of Super-Imposed Synchronization Sequence Using Matched Filter. // Radioelektronika 2013: 23th Microwave and Radio Electronics Week (MAREW 2013), Pardubice, Czech Republic, April 16-17, 2013, pp.84-88.

The following papers have been published in scientific journals:

[20] Aboltins A., Misans P., Terauds M., Valters G. Initial Implementation of Generalized Haar Like Orthonormal Transforms into FPGA-Based Devices - Part I: Signal Spectrum Analyzer Synthesizer Module // RTU, Telecommunications and electronics. Vol.8 (2008), pp. 16-21

[21] Aboltins A., Klavins D. Synchronization and Correction of Channel Parameters for an OFDM-Based Communication System // Automatic Control and Computer Sciences. - Vol.44, No.3. (2010), pp. 160-170.

[15] Aboltins A. Comparison of Orthogonal Transforms for OFDM Communication System // Electronics and Electrical Engineering. - Vol.5. (2011), pp. 77-80.

[16] Aboltins, A., Misans, P. Singular Value Decomposition Based Phi Domain Equalization For Multi-Carrier Communication System // Electronics and Electrical Engineering, Vol.18, No.9, (2012), pp.71-74.

All mentioned papers are referred by various citation databases. The summary of the paper and their citation availability in databases is given in Table 1.1.

2 Baseband components

In this chapter the major components of parametric GUR-based PMC system transmitter and receiver are reviewed. Additionally, the requirements to constructions of the GD and TD signals, compatible with the proposed PMC system baseband structures, are developed.

2.1 Structure of a parametric multicarrier modulation system

Modern data communication systems contain units performing various operations in order to transmit information from a binary source to a destination. In accordance with the Open System Interconnection (OSI) architecture, any data communication system can be divided into 7 layers. Figure 2.1 depicts the major components located in the *physical layer* of a PMC communication system. The most important and complex parts of the physical layer are *baseband* units.

The baseband of the PMC system transmitter produces a low-pass signal whose lowest frequency is 0. Then, by means of RF modulator, a complex-valued baseband signal is up-converted to a real-valued passband signal. An RF signal propagates via the communication channel – air, cable, fiber etc. until reaches the receiver, which, in turn, by means of down-converter, provides conversion of a passband signal into a baseband signal. Some communication systems, for example, digital subscriber line (DSL), do not use upconversion, and low-pass signals are transmitted over the propagation media. In this case a complex signal is converted into a real one by adding of complex-conjugated subcarriers.

This doctoral thesis addresses the baseband parts of GUR-based transmitter and receiver . Moreover, in further text we are dealing with the baseband equivalent (see Section 7.1.3) of the communication channel, which includes all RF parts (quadrature modulator, physical communication channel and quadrature demodulator, see Figure 2.5).

2.1.1 Transmitter baseband

A structure of PMC system transmitter baseband is depicted in Figure 2.2.

The purpose of the first unit - the mapper is converting binary symbol groups into symbols with higher dimensions and/or larger alphabets. For instance, the mapper will map the binary combination `0111` into the complex number `-1.0000 - 3.0000i`, which is one of the `4x4=16` possible values in 16-QAM constellation.

Before entering the inverse unitary transform unit, the output vector of the mapper is mixed with transform-

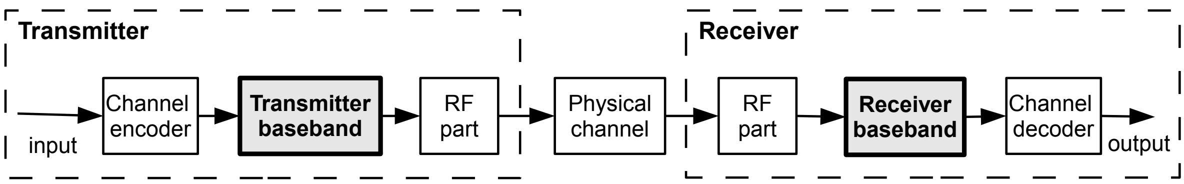

Figure 2.1: Physical layer of a communication system

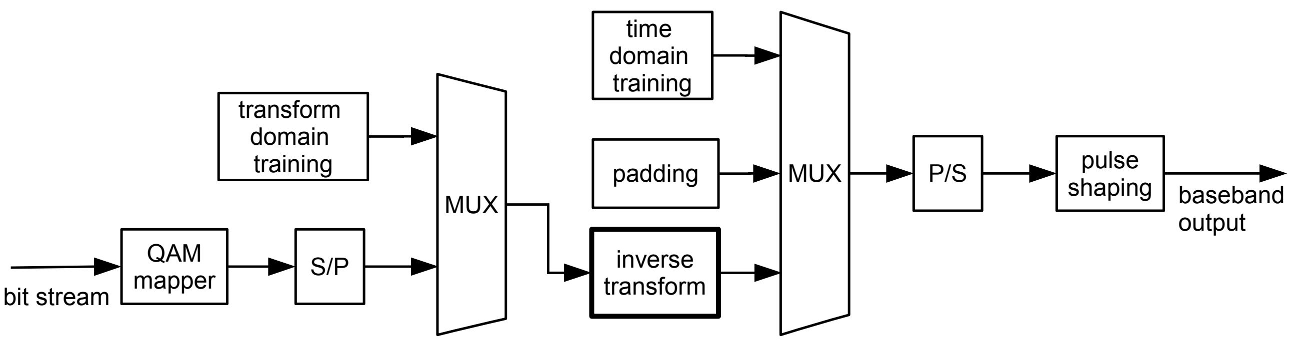

Figure 2.2: Baseband of the PMC system transmitter

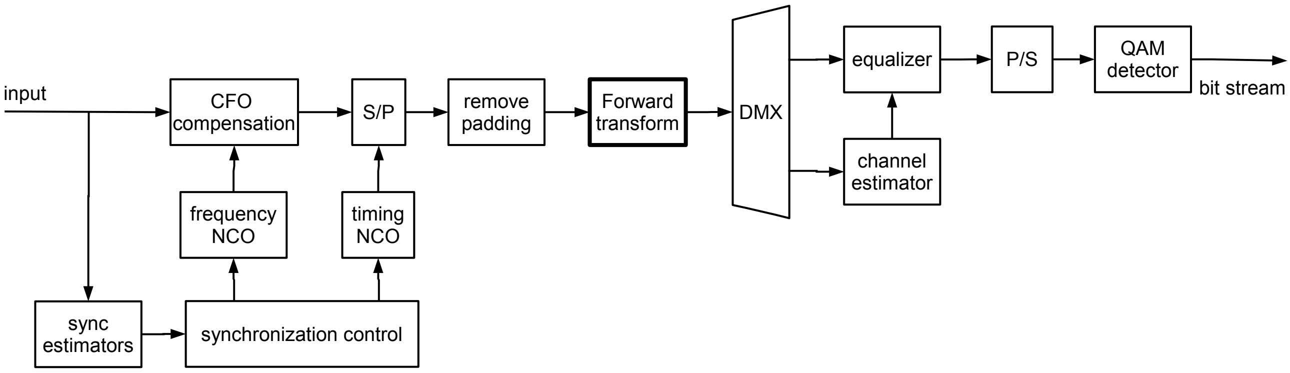

Figure 2.3: Baseband of the PMC system receiver

domain training (pilot) samples. The purpose of these special samples is to provide signals for synchronization and transform-domain (for example, FD) channel estimation.

The unitary transform (see Section 3.1) unit is one of the key elements of PMC system. The purpose of this unit is to create such set of orthogonal *subcarriers*, which is most appropriate for transmission via communication channel. In other words, the goal of the transform is to make the incoming vector space more resistant to channel effects, such as scattering, noise and attenuation. More information about the MC modulation is given in Chapter 3.

After MC modulation TD training blocks, containing training symbols are usually added. These symbols act as timing references and can be used for TD channel estimation. Moreover, padding samples like CP (see Section 2.2.4.1), UW (see Section 2.2.4.3) or zero padding (ZP) (see Section 2.2.4.2) can be added to the block at the output of unitary transform.

Finally, after output samples are converted into serial form [1] (not shown), they are filtered with the pulse shaping filter (see Section 2.4).

2.1.2 Receiver baseband

The structure of PMC system receiver baseband is depicted in Figure 2.3 and it resembles typical MC receiver architectures. Notice, that because of the necessity to perform synchronization and equalization, the receiver structure is much more sophisticated than that of the transmitter .

After down-conversion, a baseband signal enters the internal receiver. A TD signal is being split here into two branches: main branch for useful information extraction and synchronization branch for synchronization and TD channel estimation. Early synchronization extraction is necessary, because the receiver is unable to perform any operation in the main branch until at least coarse timing and frequency synchronization is established. Thus, the purpose of the “sync estimators” unit is to obtain initial timing and frequency synchronization. Later, when the received signal will be equalized, more precise synchronization will be possible.

Timing and frequency synchronization is performed by means of two numerically controlled oscillators (NCOs). First, the frequency NCO generates a signal, which is being multiplied with the received signal in the unit “carrier frequency offset (CFO) compensation” for CFO (see Section 5.1.1) correction. The second NCO generates pulses, which direct the serial to parallel (S/P) converter and create blocks of samples from the serial stream. It is necessary to obtain correct block synchronization (see Section 4.2) in order to separate blocks correctly.

Before forward transformation, the block padding, which is used for synchronization, estimation and IBI reduction can be removed. The forward transform unit (see Section 3.1) performs one of the major operations - demodulation of the subcarriers.

After forward transformation into the transform domain, channel estimation (see Section 6.4) and equalization (see Section 6.5) take place. The purpose of the equalization is to eliminate inter-symbol interference (ISI) and ICI, introduced by the communication channel. The purpose of the “channel estimator” unit is to estimate characteristics of the baseband equivalent of the communication channel (it runs from the inverse transform unit in the transmitter to the forward transform unit in the receiver).

The quadrature amplitude modulation (QAM) detector performs inverse operation of the mapper – converts

[1] in some cases it is not necessary, see Section 3.2.3

complex modulation symbols into binary digits. It has to be noticed, that QAM detection is a much more sophisticated operation than QAM mapping, since samples at the input of the detector can be strongly corrupted by the noise, ICI and ISI. Detection is based on selection of a constellation point with a minimal distance to the received sample.

2.2 Structure of baseband signals

Since unitary transformation is used for subcarrier modulation, GD and TD samples are grouped into blocks. Grouping is performed before the unitary transformation.

In the baseband part of the PMC system transmitter , complex-valued data symbols manipulate N discrete basis functions $\varphi(n,k)$ of unitary transformation $\mathbf{\Phi}$, where n is the subcarrier index (in the transform domain) and k is the sample index (in the TD).

2.2.1 Equation form

Subcarrier manipulation and transformation from the transform domain to the TD are given as:

$$x(k) = \frac{1}{\sqrt{N}} \sum_{n=0}^{N-1} X(n)\varphi^{-1}(n,k), \quad k = 0, 1, ..., N-1, \tag{2.1}$$

where $X(n)$ is the useful information samples and N is the size of the information block. These transform domain samples are, in fact, spectrum coefficients. TD waveform $x(k)$ sent over the communication channel becomes corrupted and the received TD signal is given by:

$$y(k) = \sum_{m=0}^{M-1} h(m)x(k-m) + w(k), \tag{2.2}$$

where h is the impulse response of the channel with length M and w is an additive noise. Received transform domain samples are obtained using a forward transform of the received TD samples:

$$Y(n) = \frac{1}{\sqrt{N}} \sum_{k=0}^{N-1} y(k)\varphi(n,k), \quad n = 0, 1, ..., N-1. \tag{2.3}$$

2.2.2 Matrix form

An information block $\boldsymbol{X}$ originally is located in the transform domain. Before transmission, the inverse unitary transform brings it from the transform domain to the TD:

$$\boldsymbol{x} = \mathbf{\Phi}^{-1}\boldsymbol{X} \tag{2.4}$$

The communication channel distorts transmitted blocks $\boldsymbol{x}$ by convolution and additive noise:

$$\boldsymbol{y} = \boldsymbol{h} * \boldsymbol{x} + \boldsymbol{w} = \boldsymbol{H}\boldsymbol{x} + \boldsymbol{w}, \tag{2.5}$$

where $\boldsymbol{h}$ is the channel impulse response and $\boldsymbol{H}$ is the TD channel matrix. If the channel is static and linear, then $\boldsymbol{H}$ corresponds to a subset of Toeplitz matrices called *convolution matrix*. The receiver transforms received TD blocks back into the transform domain:

$$\boldsymbol{Y} = \mathbf{\Phi}\boldsymbol{y} \tag{2.6}$$

By means of equalization (see Chapter 6.5), estimates of the payload saples $\hat{\boldsymbol{X}} = \boldsymbol{A}^{-1}\boldsymbol{Y}$ are obtained, where $\boldsymbol{A}^{-1}$ is the GD equalization matrix.

2.2.3 Block framing

In a PMC system TD information blocks are being transmitted serially – one after another. However, for synchronization and signaling special synchronization blocks can be inserted. Moreover, transmission may be performed via asynchronous packets of blocks. In all these cases an additional TD level of aggregation arises – blocks are grouped into frames. In Figure 2.4 a typical structure of a TD signal for block-wise transmission is shown.

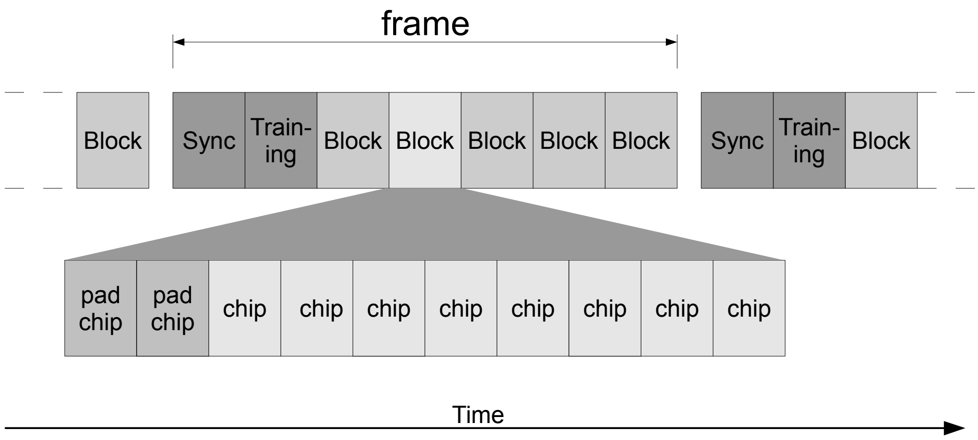

Figure 2.4: General structure of a TD signal

2.2.4 Block padding

In order to mitigate IBI, TD blocks of the samples are padded by certain patterns. Moreover, padding patterns can be used also for synchronization and channel estimation. The most widely used padding patterns are:

- Cyclic prefix (Section 2.2.4.1)
- Zero padding (Section 2.2.4.2)
- Unique word (Section 2.2.4.1)

2.2.4.1 Cyclic prefix

When a signal (2.1) is transmitted along a channel with timing dispersion, a partial superposition of adjacent blocks, i.e., ISI, can occur. Peled and Ruiz in [22] suggested using cyclic continuation of blocks – a CP – for solving this problem. The whole block $\boldsymbol{x_{cp}}$ with a CP of length L is is obtained from the TD block $\boldsymbol{s}$:

$$\boldsymbol{x_{cp}} = [s_{K-L+1}, s_{K-L+2}, \ldots, s_K, s_1, s_2, \ldots, s_K] \tag{2.7}$$

CP plays a crucial role in FD equalization (see Section 6.5) for OFDM systems. If the length of CP is greater than the pulse response of the channel, then the ISI is completely resolved by a proper choice of the time for the beginning of the block, i.e., by block synchronization (see Section 4.2).

However, in accordance with simulation results presented in [15], CP in a GUR-based PMC system does not provide those advantages available in OFDM.

2.2.4.2 Zero padding

ZP is the simplest padding method, based on padding of the transmitted vector $\boldsymbol{s}$ with zeros:

$$\boldsymbol{x_{zp}} = [0, 0, \ldots, 0, s_1, s_2, \ldots, s_K] \tag{2.8}$$

ZP provides a guard interval (GI), which prevents IBI. ZP is an energy-efficient kind of padding, since it does not require additional energy for the transmission. However, ZP provides too few facilities for synchronization and channel estimation.

2.2.4.3 Unique word

UW is a padding method where each block of samples $\boldsymbol{s}$ is preceded by a constant combination of samples $\boldsymbol{u}$:

$$\boldsymbol{x_{uw}} = [u_1, u_2, \ldots, u_L, s_1, s_2, \ldots, s_K] \tag{2.9}$$

UW is usually known to the receiver and can provide means for channel estimation (see Section 6.4) and synchronization (see Chapters 4 and 5). The UW-based padding for MC communications has many advantages. The possibility to choose between specialized sequences for synchronization and the possibility to use them for channel estimation in many cases make the UW-based padding an optimal choice.

2.3 Synchronization sequences

A PMC receiver must perform sampling of the received analog signal, must detect the start and the end of transmission and must be able to extract various service-related information from the received signal. All synchronization methods can be classified by technique, domain and structure.

In order to provide DA or DD timing and frequency synchronization as well as *channel estimation* sequences must be added to the useful signal. In an ideal case, the same sequence is used simultaneously for timing/frequency synchronization and channel estimation.

2.3.1 Adding and removal of synchronization sequences

There are several ways how a synchronization sequence can be embedded into a transmitted signal. Two most popular ways of super-position between the payload signal and the synchronization signal are *inserted sequence* and *SI sequence* .

2.3.1.1 Inserted sequences

Synchronization and training sequences are placed between the useful samples. A UW prefix is a typical example of an inserted synchronization sequence. Once correct timing offset synchronization (see Chapter 4) is established, inserted sequences can be easily removed by discarding respective samples of the received signal. The major drawback of the inserted sequences is that they consume time and frequency resources, since during transmission of synchronization sequences no payload is being transmitted.

2.3.1.2 Super-imposed sequences

SI sequences are added to the useful signal. They can provide a considerable bandwidth saving, since they consume just a small portion of the dynamic range of the signal rather than time or frequency resources.

Unlike inserted sequences, SI sequences cannot be easily removed. The typical approach is based on subtraction of the synchronization sequence from the received signal. However, this approach works only in case of good equalization (see Chapter 6). Moreover, the magnitude of super-imposed sequence (SIS) must be known.

In this doctoral thesis and in paper [19] it is described how to exploit the randomness of the useful MC signal in order to remove the SI sequence without the knowledge of its amplitude . For example, OFDM is frequently treated in literature as a complex random process having a circular symmetric complex normal (Gaussian) distribution [23]. Therefore, the correlation of MC signal with any other independent signals will be weak and the orthogonality will increase along with the number of subcarriers. There are two filtering approaches described:

- using GUR;
- using a matched filter (MF).

The second filtering approach reduces to finding the inner product between the SIS $\boldsymbol{u}$ and the received signal $\boldsymbol{y_{si}}$:

$$\boldsymbol{y} = \boldsymbol{y_{si}} - \frac{\boldsymbol{u}^* \boldsymbol{y_{si}}}{||\boldsymbol{u}||^2} \boldsymbol{u} \tag{2.10}$$

2.3.2 Review of the UW sequences

2.3.2.1 Zadoff-Chu sequence

In article of Chu [24], the approach of generating codes with good periodic correlation properties is described. These sequences represent so -called constant amplitude zero autocorrelation (CAZAC) sequences. The codes are generated using the following equations:

$$a_k = \begin{cases} e^{j\frac{M}{Q}\pi k^2}, & \text{if Q is odd} \\ e^{j\frac{M}{Q}\pi k(k+1)}, & \text{if Q is even} \end{cases} \tag{2.11}$$

where $k = 0, 1, \ldots, Q-1$ is the sample index, M is an integer *coprime* with Q.

2.3.2.2 Schmidl-Cox sequence

In the widely-cited paper [25] by Schmidl and Cox, the authors propose to use two special training blocks. The first block in the TD consists of two equal parts. It is generated by filling even subcarriers with a complex pseudo-noise (PN) sequence and setting odd subcarriers to zero. The symmetry of the block makes it immune

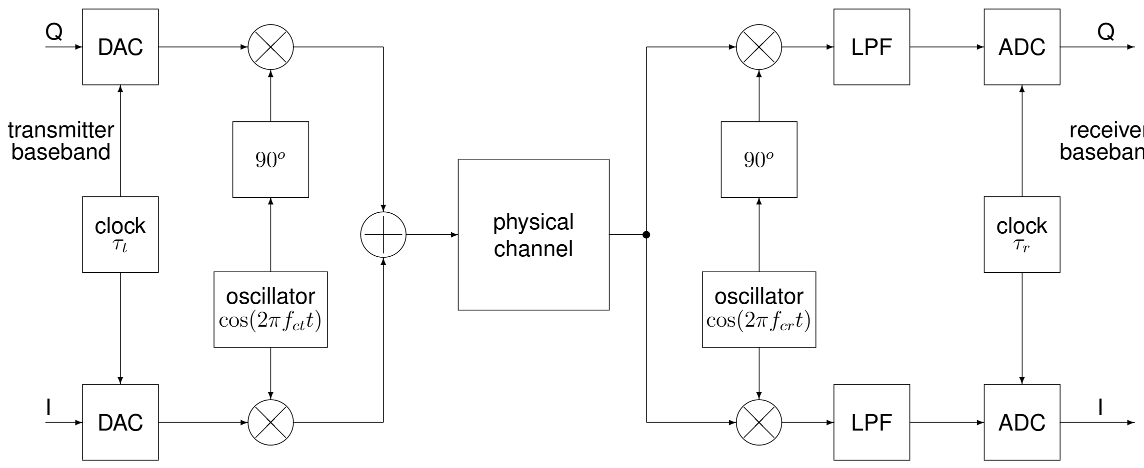

Figure 2.5: RF part of a PMC system

to carrier and sampling frequency offsets and makes possible fast detection of the block start. Moreover, the values on even subcarriers allow to make FD channel measurements. The second block consists of two another PN sequences. They will help to measure the channel frequency response on the remaining (odd) frequencies and to calculate the frequency offset.

2.3.3 Impact of the communication channel on training sequences

Dispersion in the communication channel and pulse shaping filters corrupts the training sequences designated for time and frequency synchronization. It is of big importance to understand how channel effects, namely convolution, impact the amplitude and phase of autocorrelation (AC) and cross-correlation (XC). The experimental results provided in this doctoral thesis show that:

- Convolution in the communication channel significantly affects the XC properties of training sequences. Namely, the XC function of the received signal is equal to the convolution between AC function of the transmitted signal and reversed channel impulse response.
- Stationary convolution of the shaping filters and time-dispersive communication channel does not have a strong impact on the AC properties of training sequences. Therefore, AC can be used as a robust method for estimation.

2.4 Transmit filtering and upconversion

A serialized complex signal at the output of parallel-to-serial (P/S) converter has the sampling rate F_{chip}, which is N times higher than the speed of the unitary transform unit. Before transmission over the communication channel digital complex samples must be converted to an analog signal and upconverted to the carrier frequency (in case of passband transmission) or converted into a real-valued signal (if baseband transmission is used).

Additionally, before *upconversion* a signal must be filtered in order to eliminate harmonics created by the transitions between the samples, i.e. sample rate conversion of the signal is necessary. Unfortunately filtering, which uses convolution of TD signal, leads to ICI in the GD.

Upconversion can be performed by standard means of quadrature modulation – the real part of the signal is modulated by $cos(2\pi F_c t)$, whereas the imaginary part by $sin(2\pi F_c t)$. By F_c in this formula the carrier frequency is denoted. In practical implementations it is important to choose a carrier frequency generator with low phase noise and high frequency stability, since MC systems are very sensitive to frequency offsets (see Chapter 5). The RF part of a PMC system with upconversion is depicted in Figure 2.5.

Conclusions

- CP cannot be used within GUR-based PMC systems, because it do not mitigate ICI.
- UW prefix is suitable for use in GUR-based PMC systems.
- SIS is an alternative method for the transmission of training and synchronization sequences in MC communication systems.
- Convolution in the communication channel seriously affects XC properties of the received signal.
- Pulse shaping filter at the transmitter baseband output causes ICI.

3 Multicarrier modulation

This chapter is devoted to exploration for MC *modulation* and *demodulation* based on GUR.

3.1 Unitary transforms for digital modulation

In order to provide a MC modulation, unitary transforms can be used (see Section 2.2). Although there is a large variety of known unitary transforms, only few of them are used for the creation of the subcarriers in MC modulation. The most popular unitary transforms used for this purpose are:

3.1.1 Identity transform

Transformation matrix of the identity transform is represented bu the Identity matrix. Since there is no any signal transformation, plain QAM signal is transmitted between transmitter and receiver.

3.1.2 Fourier transform

A typical example of block transmission technique, employing Fourier transform is OFDM. BFs of discrete-time equivalent of the Fourier transform, called DFT are defined as follows:

$$\varphi(k,n) = e^{-j2\pi k\frac{n}{N}} \tag{3.1}$$

3.1.3 Complex Hadamard transform

Complex Hadamard transform basis functions $\varphi(n,k)$ are columns of Hadamard matrix [26]. Hadamard transform, which consists of *real* values only, is also known as WHT.

$$\boldsymbol{\Phi_1} = \begin{bmatrix} 1 & -j \\ 1 & j \end{bmatrix} \tag{3.2}$$

$$\boldsymbol{\Phi_n} = \boldsymbol{\Phi_1} \otimes \boldsymbol{\Phi_{n-1}} = \boldsymbol{\Phi_1} \otimes^n \tag{3.3}$$

3.1.4 Generalized Unitary Rotation transform

GUR[1] is a technique, which allows to factorize unitary matrices using fast elementary rotations in a real or a complex signal spaces [28]. Unitary matrices can be factorized using an alternative algorithm [29] .

On the other hand, GUR provides a fast mechanism for creation of arbitrary unitary bases by means of factorization of N-dimensional (currently, 2-dimensional) rotations. Unitary transform matrix $\boldsymbol{\Phi}$ of GUR transform is defined as follows:

$$\boldsymbol{\Phi} = \prod_{p=\log_2(N)}^{1} \boldsymbol{B_p}(\phi,\gamma,\psi), \tag{3.4}$$

In this equation ϕ, γ and ψ are real angles which could take any value $\in [0; 2\pi]$, and stairs-like orthogonal generalized rotation matrix (SOGRM) $\boldsymbol{B_p}$ is defined as:

[1]Term ”GUR” has been introduced by Misans and Valters [27] and in earlier publications [28] it was called ”Phi transform”.

Acronym	Explanation
RABOT	Most general transformation, where all parameters are variable
CCRAOT	All angles are constant throughout all SOGRMs as well as inside each SOGRM (*In the thesis angle ϕ in equation 3.6 usually is written besides transform name. Default values of the other angles are $\gamma = \pi/2, \psi = 0$*).
CRAIMOT	Each SOGRM of is different, whereas inside SOGRM angles remain constant

Table 3.1: Summary about some GUR transforms.

$$
\boldsymbol{B_p} = \begin{bmatrix}
\tau^1_{1,p} & 0 \;\; 0 & \dots & 0 \;\; 0 \\
0 \;\; 0 & \tau^1_{2,p} & \dots & 0 \;\; 0 \\
\dots & \dots & \ddots & \dots \\
0 \;\; 0 & 0 \;\; 0 & \dots & \tau^1_{N/2,p} \\
\tau^2_{1,p} & 0 \;\; 0 & \dots & 0 \;\; 0 \\
0 \;\; 0 & \tau^2_{1,p} & \dots & 0 \;\; 0 \\
\dots & \dots & \ddots & \dots \\
0 \;\; 0 & 0 \;\; 0 & \dots & \tau^2_{N/2,p}
\end{bmatrix} \tag{3.5}
$$

This matrix contains mutually independent plane rotations only. However it contains just fraction of total number of rotations, thus it is necessary to factorize $\log_2(N)$ such matrices in (3.4). Elements of each SOGRM are obtained from unitary four-element single-plane rotation matrices. There are possible 64 variants (sine, cosine, + and - combinations) of single-plane rotation matrix. One variant of single-plane rotation matrix could be:

$$
\Upsilon = \begin{bmatrix} \tau^1_{q,p} \\ \tau^2_{q,p} \end{bmatrix} = \begin{bmatrix} \mp sin\phi_{q,p}e^{-j\psi_{q,p}} & cos\phi_{q,p}e^{j\gamma_{q,p}} \\ cos\phi_{q,p}e^{-j\gamma_{q,p}} & \pm sin\phi_{q,p}e^{j\psi_{q,p}} \end{bmatrix} \tag{3.6}
$$

3.1.4.1 Creation of unitary bases with desired first basis function

One of the most important applications of the GUR is creating of such unitary basis, where one of the basis functions coincides with the required waveform. If incoming vector is scaled version of one of BFs, then output of the transformation contains only one non-zero sample. Therefore, this algorithm provides an excellent facility for the compression of the signals, similar to the $\boldsymbol{U_d}$. On other hand, using this operation it is possible to super-impose required signal into the output sequence.

For the creation of a basis consisting of complex waveforms, a rotation in complex space is required. This task can be fulfilled using two real rotations [28].

Limitation of the algorithm, described in [28], is that it can process incoming vectors with number of samples, which are power of two. In some cases, for example, if just part of block should be transformed, it is necessary to process blocks, whose length is not power of two. **In this dissertation algorithm [28] was extended, in order to produce orthonormal bases, whose dimensions are any real integer**.

3.1.4.2 Classification of GUR transforms

Table 3.1, which is reprinted from [14], summarizes information about some sub-classes of the GUR transform. Figure 3.1 shows example of modulation of 16 samples using 4-carrier inverse complex constant rotation angle OT (CCRAOT).

3.2 Configurations of multicarrier modulator and demodulator

There are sevaral ways how to perform unitary transformation and MC modulation. This section is devoted to description of possible solutions for performing this task.

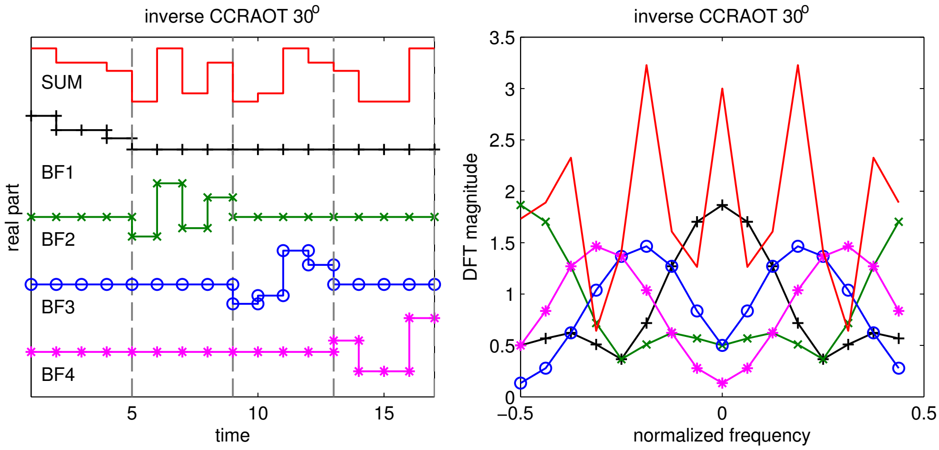

Figure 3.1: Example of transmission of 16 QAM samples 1000 0100 0010 0001 using 4-carrier MC modulation, based on inverse CRAOT 30^o

3.2.1 Parametric multicarrier modulation system with matrix-based transform algorithm

Most simple and most obvious way to perform unitary transformation is build an unit, which directly mimics unitary transformation matrix (3.4). It is possible to generate infinite number of transforms even if CCRAOT, where all angles remain the same in all matrices $\boldsymbol{B_p}$. This fact is evidence that even simplest configurations of the unitary transform unit can provide enough flexibility for the PMC system.

3.2.2 Parametric multicarrier modulation system with tree-like transform algorithm

In order to transform vector by means of unitary matrix, internal products between transformation matrix rows and the original vector are calculated. This operation can be viewed as correlation or filtering of the input signal by bank of finite impulse response (FIR) filters. Each row of the orthogonal transform (OT) thus represents a different filter. This concept has led to many interesting theories and highly efficient designs [4], especially in area related to frequency division systems, such as filtered multitone (FMT) and FBMC .

3.2.2.1 Factorization of GUR using tree-like structures

It is possible to use tree-like structures for obtaining factorization (3.4). As a basic building block Elementary Generalized Unitary Rotation (EGUR) is used. EGUR function is described by the equation (3.6). EGUR module can bee steered by the 2 parameters:

1. Forward/inverse transform (boolean);
2. Rotation angle (double);

EGUR module can be exploited as part of:

- 2D reconstruction module (2Re);
- 2D decomposition module (2De);

Input of this block is 2 serial samples, but output - 2 parallel samples. 4-dimensional decomposition can be achieved by using 3 two-dimensional `De2` units. In the dissertation a description how obtain decomposition or reconstruction trees with arbitrary size is given.

3.2.3 Transmultiplexer

In literature systems with synthesis filter banks in the transmitter and analysis filter bank in the receiver are referred as *transmultiplexers* . FMT technology is a typical example of transmultiplexer. In FMT each subcarrier is produced by the individual digital bandpass filter. Usually bandpass filters are created by combining inverse discrete Fourier transform (IDFT) and low pass filters with different phase responses. At the receiver reverse processing takes place.

In the dissertation description and block diagram of GUR-based transmultiplexer is given. Synthesis filter bank in the transmitter produces serial stream of samples at the output of unitary transform unit of the transmitter. Insertion of additional information, such as training and/or synchronization samples, in the transmitter must be done in the transform domain and any manipulations with TD signal are costly and inefficient.

The largest challenge with the transmultiplexer configuration is that all synchronization samples must be generated and added to the data in the transform domain, where samples are in a parallel form. Channel estimation (see Chapter 6.4) in transmultiplexer-based PMC system must be performed strictly in GD, since TD samples are available in serial form only and extraction of the training samples is problematic.

3.2.4 Subband coder

It is possible to interchange decomposition an reconstruction stages, i.e. place decomposition (analysis) in the transmitter of communication system and reconstruction (synthesis) - in the receiver. Such solutions are called *subband coders* . The concept of first GUR-based subband coder was proposed by Misans and Valters in [12]. Significant drawback of the proposed modulation scheme, that it is impossible to insert anything (for example transform domain training) into signal before unitary transformation. Therefore, communication system, based on subband coder must exploit TD training structures in order to avoid S/P-P/S conversion usage, which will increase latency of the communication system. Receiver side processing also has to be adjusted for utilization of reconstruction unit. Main challenge in this case is equalization (see Chapter 6.5), since it has to be performed on a serial sample stream. Since TD training structures are recommended for the efficient transmission, channel estimation in the TD is recommended.

3.2.5 Performance comparison of multicarrier modulators: simulation results

Using numerical simulations, all three types of transform units has been compared. PMC systems with ideal timing and frequency synchronization and additive white Gaussian noise (AWGN) communication channel has been simulated. Although differences are insignificant, subband coder shows little better results.

Please notice, that AWGN channel has been used in the simulations. In case of dispersive channel, difference would be more significant. However, since dispersive channel requires equalization, which is not available for tree like structures yet, this question remains open.

3.3 Peak-to-average power ratio of the multicarrier signal

Since MC signal consists of several waveforms added together, it can have a noticeable envelope variations. Ratio between peak power and average power of the signal is called PAPR. PAPR (in dB) of continuous signal $s(t)$ is defined as follows:

$$\beta = 10log_{10}\frac{\max[s^2(t)]}{E[s^2(t)]} \tag{3.7}$$

System performance degradation due nonlinearities of communication equipment have larger effect on signal with larger PAPR. Moreover, large PAPR requires amplifiers with a high dynamic range and large power consumption.

Complementary cumulative distribution function (CCDF) function of the signal can be used to explore variations of the instantaneous power of the signal. In Figure 3.2 CCDFs of instantaneous power of signal of several MC signals, created by various transforms and 4QAM constellation, are compared. From this plot we can observe long tail of CCDF of OFDM signal, created by the DFT. Moreover, CCDF of complex Hadamard (see Section 3.1.3) and CCRAOT with angles $> 20^o$ is very similar to CCDF of OFDM signal, based on DFT. This observation allows to conclude, that PAPR of those signals is similar to PAPR of OFDM. From the same figure can be observed that PAPR of small angle CCRAOT is significantly lower. Finally, CCRAOT 0^o has constant power of the 4QAM signal, since transformation matrix of CCRAOT 0^o is equal to Identity matrix.

3.3.1 PAPR reduction using super-imposed sequences

In accordance with numerous researches, the utilization of SI training signals can lead to reduced PAPR of the transmitted signal. Selecting of SIS with a low PAPR leads to reduction of PAPR in the summary signal. Good candidates for PAPR reduction are maximum length sequence (MLS) (m-sequence) or CAZAC sequences, for example a Zadoff-Chu (ZC) sequence.

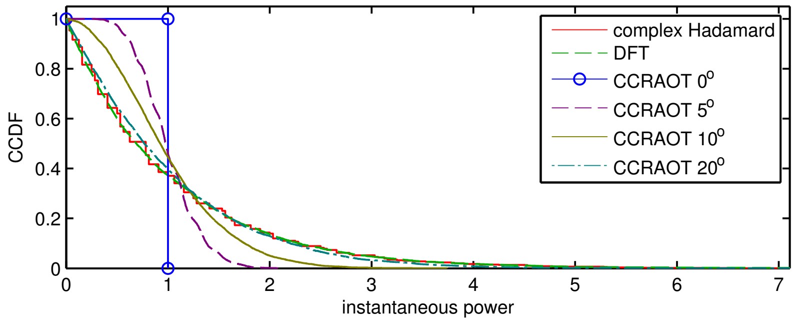

Figure 3.2: Comparison of CCDFs of MC signals, created by various transforms and 4QAM constellation.

3.4 Transform selection for the parametric multicarrier modulation system

Using GUR mechanism it is possible to construct an infinite number of unitary transformations. By looking to all variety, a natural question arises "How to construct an optimal transform?".

Since ultimate goal of any data communication system is to provide maximum data rate in a given frequency band and consume as less power as possible, selection of basis function set must lead to the satisfaction of those conditions. There are several factors, which affect throughput and power consumption and, therefore, selection of the transform:

- Transform can be selected in accordance with channel state information (CSI)(see Section 6.4). Oka and Fossorier [11] used angular matrix similar to (3.5), to construct orthogonal transform family. They experimentally proved, that performance of the communication system with non-Gaussian communication channel depends on angles – some combinations of angles performed noticeably better.
  Doctoral dissertation [9] is devoted to time-frequency representation of non-stationary, i.e. changing in time environments, using Weyl-Heisenberg expansions. Work provides background for the building of filter banks, including GUR-based ones, which will perform optimally in these non-stationary environments.
- Transform can be selected in order to minimize impact of interference. For example, if one of the basis functions will coincide with periodic interfering signal, then impact of the external interference will be limited to just one subcarrier and PMC system will continue to work even if signal-to-interference ratio (SINR), i.e. ratio between useful signal power and interference power, will be -20dB. It must be noticed, that in this case the length of the block as well as a phase of transmitted signal must be adjusted in order to obtain a perfect removal of the interference. Figure 3.3 (left) shows impact of the random periodic broadband noise in the communication channel on performance of OFDM and GUR-based system, which uses basis function set, where one of the basis functions coincides with the undesired periodic signal (see Section 3.1.4.1).
- Synchronization accuracy can affect selection of the transform. Basis functions with compact time and frequency supports, like wavelets in FBMC systems, can reduce ICI and sensitivity to the CFO.
- As it was said, using GUR, it is possible to obtain large variety of transforms. If receiving side do not know parameters of the transform, it is unable to decode the received information. This feature can be used fo creation of secure and even masked PMC systems. Figure 3.3 (right) shows results of an experimental examination of a *angle resonance* in PMC system with transmitter using CCRAOT 30^o. It can be seen, that receiver is able to work if angle error do not exceed approximately 8^o.
- Signals with large PAPR require large RF amplifier backoff, which leads to the increased power consumption. Using parameters of GUR, it is possible to change PAPR of the signal in the wide range. More details about this feature is given in Section 3.3.

3.4.1 Parametric communication systems

One of the key advantages of the GUR transform is that it can be completely described, i.e. parametrized, by set of the angles. This feature make GUR especially suitable to the communication systems, where transform changes dynamically, in accordance with current situation. **Since, the transform in the transmitter and the receiver must be changed simultaneously, along with other information, parameters of the transform**

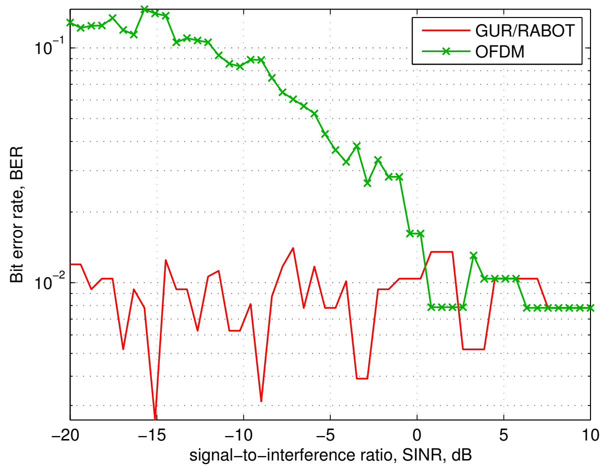

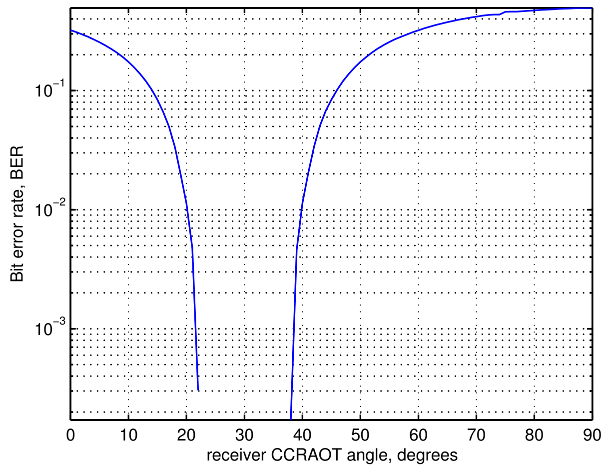

Figure 3.3: Impact of a random periodic 64-sample signal to OFDM and specially tuned GUR-based PMC systems both having 64 subcarriers (left). Angle resonance in PMC system with transmitter using CCRAOT 30^o(right)

must be continuously transferred. For signaling of the new transform, special block prefixes of frames (in case of a slower changes) must be used. Since, in many cases a *feedback* from the receiver to the transmitter is required, the proposed communication systems can be regarded as *communication systems with a limited feedback* [30].

Many of the criteria, mentioned in Section 3.4 can be changing and periodic adjustment of the transform would improve the performance of the communication system. For example, CSI and interference tend to change over time. Moreover, transform can be changing periodically, thus providing extra diversity and security.

Conclusions

- In a communication system with a AWGN communication channel performance of block type and tree-like GUR transform units is almost equal (see Section 3.2.5);
- Tree-like configurations require special synchronization and equalization methods working with a serial stream of samples.
- In range of angles between 0^o and 45^o PAPR of CCRAOT based MC TD signal is proportional to the angle.
- Particular GUR-based transform can be selected in accordance with channel impulse reaction, minimum interference, synchronization accuracy, security requirements, channel non-linearity.

4 Timing offset synchronization

The purpose of this chapter is to review existing timing offset synchronization methods and verify their applicability and limitations regarding the GUR-based PMC systems. New BTO estimation algorithms are described.

4.1 Overview

The oversampled serial stream of samples at the receiver input must be divided into information units – chips, blocks and frames. In order to divide the stream at correct positions, it is necessary to estimate relative time instants, where various information units begin. Moreover, if the current timing position is known, it is possible to predict future time instants, when the separation must be done. The task, which is responsible for the estimation of current timing position, is called *timing offset estimation* . There are several well-known timing offset estimation techniques:

- DA estimation, based on the correlation between repetitive parts, i.e. AC;
- DD estimation, based on an MF, i.e. XC;

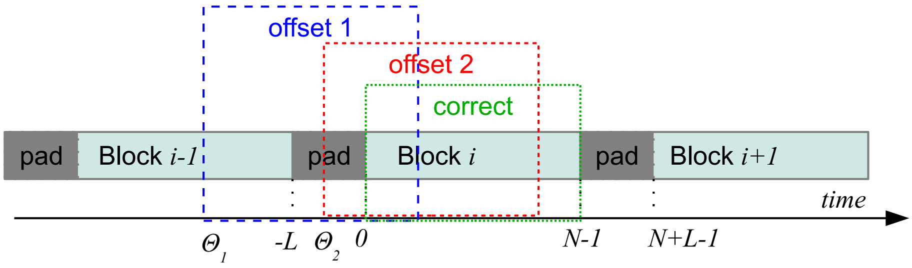

Figure 4.1: Types of BTO

- non data-aided (NDA) estimation, based on deducting the timing offset from disturbances of the received signal.

Most of the existing timing estimators for OFDM [23] are based on AC of CP. Unfortunately, CP is inefficient (see Sections 2.2.4.1 and 6.5.2) in systems based on non-sinusoidal basis functions.

Another widely used method for timing synchronization is based on XC in conjunction with UW. In SC systems UWs traditionally have been used for frame synchronization. On the other hand, in many recent publications there are proposals to use UW instead of CP in OFDM communication systems. However, UW synchronizers are usually used in conjunction with other – fine synchronization methods. Many of fine synchronization methods rely on FD information, which is not available in GUR-based PMC systems.

4.2 Block synchronization

A received serial stream of chips must undergo S/P conversion before forward transformation. The dividing of the stream must be done at correct positions, otherwise demodulation of data symbols (2.6) by means of the unitary transform unit based on the factorized matrix (3.4) will be impossible.

4.2.1 Impact of block timing offset

The BTO is a severe issue in MC communication systems. In case of block padding (see Section 2.2.4), incorrectly detected block boundaries can lead to two different situations: transformation of two incomplete sample blocks separated by the padding or transformation of an incomplete block with a part of the padding (see Figure 4.1).

In OFDM the second type of BTO is efficiently mitigated, because CP is used as padding. Due to the properties of DFT, a cyclic shift of the input vector does not lead to ICI (See Section 6.3.2) and, therefore, can be efficiently corrected by the frequency domain equalizer (FDE), which is able to estimate the communication channel *irrespective of the BTO*. Since GUR-based PMC systems use the UW padding, block synchronization is necessary before the equalization the received signal. Therefore, GUR-based PMC systems are sensitive to both types of block offsets and **block synchronization with one sample accuracy is necessary**.

4.2.2 BTO estimation

4.2.2.1 Data-aided block timing offset estimation

DA estimators rely on the signal structure in order to obtain necessary information. Autocorrelation between repeating parts is a typical example DA estimation.

In OFDM literature several simple DA methods for BTO estimation are described. If the communication system uses CP (see Section 2.2.4.1), there are several ways for determining the bounds of symbols. The authors of early papers (Tourtier et al., 1993) suggested using the absolute value of the difference between the signal and its copy delayed by N samples. Other authors in a more recent study [23] have suggested using of AC:

$$v_{ac}(k) = \sum_{m=k}^{k+L-1} y(m)y^*(m+N),\ k \in \{0, ..., \theta, ...N+L-1\} \tag{4.1}$$

In this case the estimate of the block delay can be found using:

$$\hat{\theta}_{ac} = \arg\max_{\theta}\{v_{ac}(\theta)\} \tag{4.2}$$

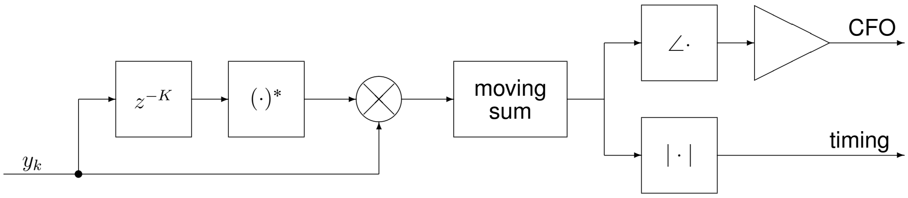

Figure 4.2: Combined AC-based BTO and FCFO estimator

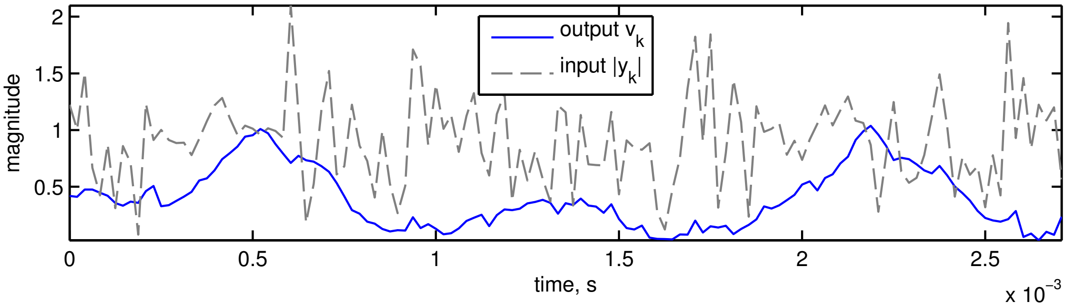

Figure 4.3: Signals in the UW AC-based estimator

Data-aided BTO estimation in GUR-based PMC systems

The experimental results published in [15] have confirmed, that CP does not provide those advantages available in OFDM. As an efficient alternative, the UW padding (see Section 2.2.4.3) has been selected. Since UW is repeated in each block, many AC-based methods for CP (see Section 2.2.4.1) can be adopted for UW. The block diagram of a BTO and FCFO (see Section 5.3.1.1) estimator based on AC is depicted in Figure 4.2. Its operation is based on Formula (4.1).

Although such synchronization estimator itself is relatively simple, unlike an XC-based estimator (see Section 4.2.2.2), its output is not suitable for direct keying of S/P conversion block. An AC-based estimator (4.1) outputs slowly varying result of multiplication (see Figure 4.3). Maximums of v_k (see Figure 4.3) must be tracked in order to obtain correct block synchronization metrics. Moreover, the search must be performed over the whole block time interval to ensure obtaining of the global maximum (v_k can have several local maximums). The result of this tracking operation is BTO, which can be used for the control of timing NCO (see Section 4.2.3).

Maximum likelihood AC-based block timig offset estimator

The above-described simple timing estimator is sub-optimal, since it does not take into account the statistical properties of synchronization sequences. The maximum likelihood (ML) estimation technique is widely adopted in many BTO estimators for OFDM.

A well-known method of deriving an optimal ML estimator for timing and frequency synchronization in OFDM systems using CP is presented in [23]. In the doctoral thesis this method is adopted to systems using a complex normally distributed UW. The proposed ML estimation method is built upon the statistic (4.1) in conjunction with an additional statistic as follows:

$$a(m) = \frac{1}{2}\sum_{k=m}^{m+L-1} |y(k)|^2 + |y(k+N)|^2, \tag{4.3}$$

which leads to a combined estimate for the delay of the blocks represented in the form:

$$\hat{\theta}_{ML} = \arg\max_{\theta}\{|y(\theta)| - \rho a(\theta)\}, \tag{4.4}$$

where

$$a(m) = \frac{1}{2}\sum_{k=m}^{M+L-1} |y(k)|^2 + |y^*(k+N)|^2 \tag{4.5}$$

$$\rho = \frac{\sigma_s^2}{\sigma_s^2+\sigma_n^2} = \frac{SNR}{SNR+1} \tag{4.6}$$

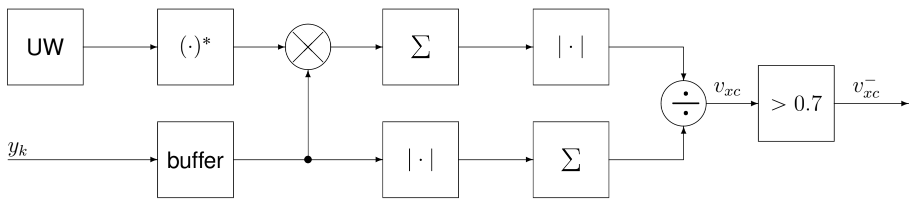

Figure 4.4: XC-based BTO estimator

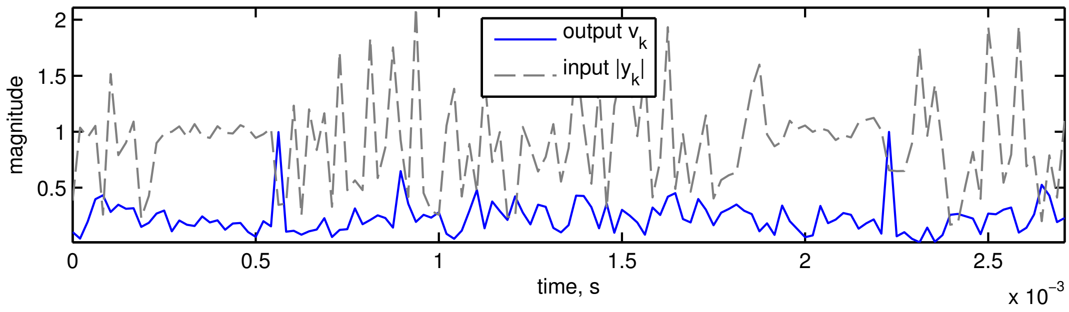

Figure 4.5: Signals in the UW XC-based block sync estimator.

and σ_s and σ_n are respective standard deviations of UW and noise.

4.2.2.2 Decision-directed block timing offset estimation

XC-based estimators are typical examples of DD estimators, i.e. such estimators, where the content of synchronization sequence plays a crucial role. XC-based estimators are widely used for frame (see Section 4.3) and start-of-packet detection.

Cross-correlation-based BTO estimation in GUR-based PMC systems

If equal UW sequences are placed in each block, a direct low-complexity XC-based BTO estimator can be designed. If we denote received samples as y and known UW samples as u, then the correlation operation will be described by the following equation:

$$c_{xc}(k) = \sum_{m=1}^{L} y(k+m)u(m)^* \ , \tag{4.7}$$

where L is the total length of UW padding and $(\cdot)^*$ denotes the complex conjugation. In order to provide normalization, it is necessary to divide the obtained result with the mean magnitude of the incoming signal:

$$v_{xc}(k) = \frac{c_{ac}(k)}{\overline{y(k)}} = \frac{\left|\sum_{m=1}^{L} y(k+m)u(m)^*\right|}{\sum_{m=1}^{L} |y(k+m)|} \tag{4.8}$$

A time delay estimate can be found by taking argument of cross correlator output samples v_{xc} with the magnitude larger than a certain threshold v_{xc0}:

$$\hat{\theta}_{xc} = \arg_{\theta}\{v_{xc}(\theta)\}\Big|_{v_{xc} > v_{xc0}} \tag{4.9}$$

The diagram of the unit providing XC-based timing estimation is given in Figure 4.4. If appropriate UW sequences are used (see Section 2.3), this algorithm outputs a sharp, one sample long peak at the beginning of each block (see Figure 4.5).

4.2.2.3 Combined block timig offset synchronizer

An AC-based estimator provides just approximate boundaries of blocks, whereas an XC-based estimator outputs a peak at the beginning of the UW sequence very precisely. On the other hand, an XC-based estimator is more sensitive (see Section 2.3.3) to additive noise and convolution in the communication channel and pulse

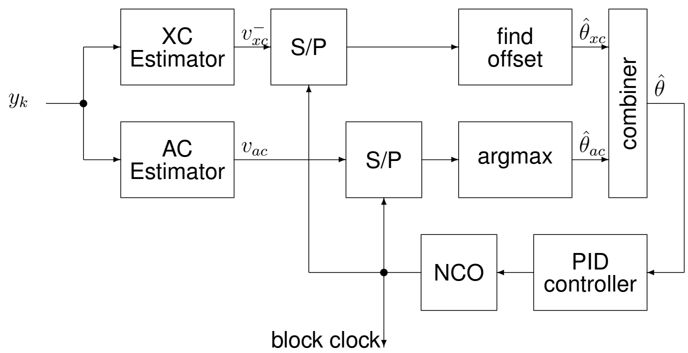

Figure 4.6: Block synchronizer

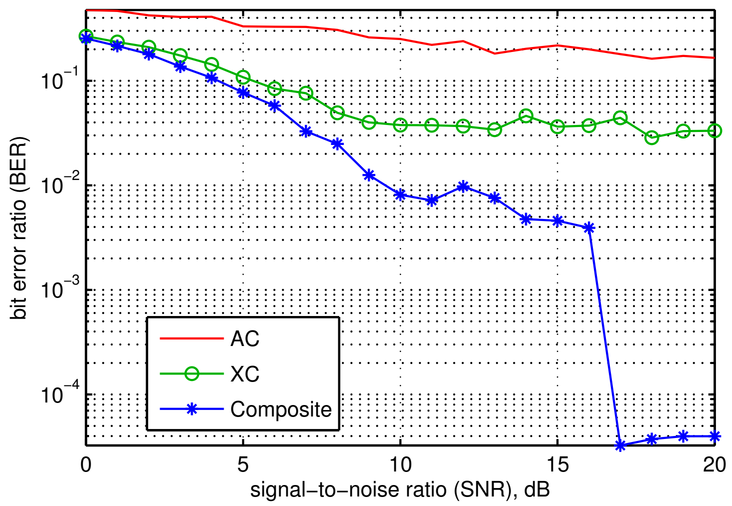

Figure 4.7: Performance of the block timing offset synchronizer using various estimators

shaping filters than a less precise AC-based estimator. Since outputs of the estimators can significantly differ, a smart combining is necessary. A combiner, which selects the estimate with the minimum magnitude, improves the performance of the synchronizer (see the simulation results in Figure 4.7).

4.2.3 Block timing offset correction

A BTO synchronizer can be implemented using two different approaches:

- Feedback (closed-loop) synchronizer: the estimator is located after the S/P converter and detects the *residual* timing offset. The detected offset via the control unit adjusts NCO, which affects the residual timing offset. The system operates in loop mode and adjusting can take *several cycles*.
- Open-loop synchronizer: the estimator is located before the main S/P converter. It inserts or deletes the required number of samples in order to achieve the breaking of the serial stream at correct positions and to obtain *immediate* synchronization.

Simulation results of the synchronizer

The performance of the above-described methods have been evaluated using simulations. For this purpose a model of baseband PMC system without equalization was created. The BTO synchronizer was implemented in accordance with the design depicted in Figure 4.6 and it uses proportional integral derivative (PID) controller. 10^6 bits were transmitted using 64 subcarriers produced by 30° CCRAOT (see Section 3.1.4.2) through an AWGN channel.

For adjusting NCO, which produces clock signal for S/P converter at the input of the receiver, PID controller can be used. Figure 4.6 depicts structure of the synchronization unit.

After careful tuning of the PID controller, the system demonstrated a stable convergence to synchronized state within approximately 20 blocks. The achieved BER in synchronized state is presented in Figure 4.7.

4.3 Frame synchronization

Most of the modern block transmission oriented systems employ framing of the block flow. Signaling information and pilot blocks for channel estimation (see Section 6.4) are commonly located at the beginning of a frame. Frame synchronization is required in order that the receiver can be able to determine the beginning of the next frame.

4.3.1 Frame timing offset estimation

The most obvious way to provide frame timing synchronization is to insert special framing signals (synchronization sequences – see Section 2.3) into a transmitted signal. Then, similar methods as for BTO estimation (see Section 4.2.2) can be used. Similar synchronization sequences can be used for frame timing offset estimation in GUR-based PMC systems, too.

4.3.2 Frame timing offset correction

For the frame offset correction the same methods as for BTO correction (see Section 4.2.3) can be used. However, since frames are much longer than blocks, the loss of the synchronization frame has a much larger impact. Therefore, open-loop synchronization methods, which provide instant synchronization, are preferred.

Conclusions

- In a PMC system the BTO can be successfully estimated, if the received signal contains a repeating UW sequence at the beginning of each sample block.
- CCRAOT-based PMC system demonstrates high sensitivity to the BTO, a delay in one chip leads to an unrecoverable loss of data. Development of shift-invariant transforms using GUR would lead to much better immunity to timing synchronization errors.
- AC-based BTO estimator provides robustness against false detections, however, its accuracy is insufficient for synchronization within one chip range.
- XC-based BTO offset estimator provides sufficient accuracy for synchronization within one chip range. However, its performance noticeably degrades in PMC systems with frequency-selective channels.
- Combination between AC-based and XC-based BTO estimators provides high accuracy and is immune to the dispersion in the communication channel.

---

5 Frequency synchronization

The purpose of this chapter is to explore the problem of frequency synchronization in MC communication systems, where subcarriers are created using GUR.

5.1 Types of frequency offset

5.1.1 Carrier frequency offset

Actual communication systems include intermediate frequency (IF) and RF sections for the translation of a signal to the required frequency (up-conversion) and back. A typical RF circuitry of the transmitter and receiver is shown in Figure 2.5. Translation is performed by two mixers and local *carrier frequency oscillator*. At the receiver side, RF demodulation is performed by means of a similar circuitry, consisting of two mixers and local oscillator. A discrepancy between carrier frequency oscillator frequencies in the transmitter and receiver leads to an effect called CFO.

A CFO projection to the *baseband* can be described as multiplication of the received baseband signal by a complex exponent with a frequency equal to the CFO:

$$y(k) = x(k)e^{j2\pi\epsilon k\tau} = x(k)e^{j2\pi\varepsilon k}\,, \tag{5.1}$$

where τ is the sample time, $\epsilon = (f_{ct} - f_{cr})$ is the absolute CFO and $\varepsilon = \epsilon\tau$ is FCFO. From Equation (5.1) it can be noticed, that the complex exponent multiplier $e^{j2\pi\varepsilon k\tau}$ is a periodic function with a period $\frac{1}{\epsilon\tau}$. Therefore, the maximum absolute CFO, which can be corrected at the baseband level, is limited to the value $\epsilon_{max} = \frac{1}{2\tau}$ and FCFO to $\varepsilon_{max} = 0.5$.

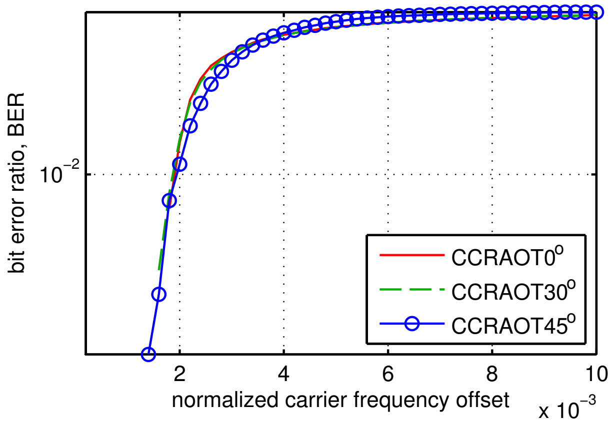

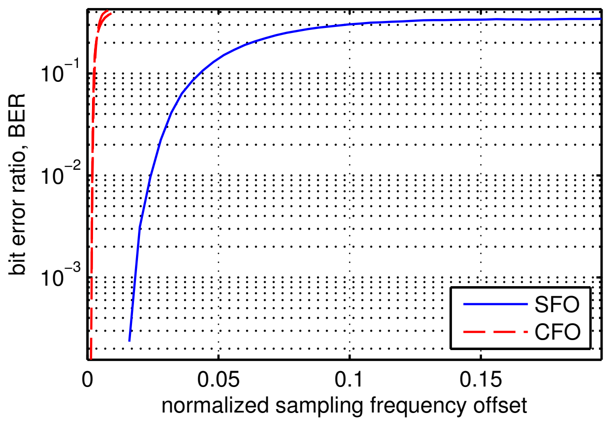

Figure 5.1: Dependence of BER on CFO and SFO in a 64-subcarrier GUR-based PMC system

5.1.2 Sampling frequency offset

In accordance with Figure 2.5, before up-conversion digital passband samples are converted into analog form by means of two digital-to-analog converters (DACs). Later, at the receiver side, they are converted to periodic discrete samples by means of two analog-to-digital converters (ADCs). Translation from digital to analog signal must be performed at the sampling frequency $f_d = 1/\tau_t$. Inconsistency between transmitter an receiver sampling frequencies causes scaling of the received TD signal:

$$y(n) = \sum_{k=0}^{D} x(k) sinc\left[\left(\frac{n\tau_r}{\tau_t} - k\right)\pi\right] \tag{5.2}$$

This effect is called sampling frequency offset (SFO). In mobile communication systems, due to the mobility of transmitter or receiver, or both, the time scale of the received signal changes. This kind of impact, known as *Doppler effect* , can be modeled as the SFO.

5.2 Impact of frequency offset

In accordance with (5.1), the effect of CFO leads to modulation of the received signal by a complex exponent. This effect can be viewed as rotation of the received samples (constellation) in the in-phase quadrature (IQ) plane. Moreover, the impact of CFO is linear and it ‘survives’ during any unitary transformation. Therefore, CFO can be estimated and corrected after the unitary transform unit of the receiver. An especially convenient situation is in OFDM, where CFO is readily available via channel estimation. Small CFOs (phase shift $\zeta < \pi/2$) can be corrected by means of *frequency* domain equalizer (see Section 6.5).

Discrepancies between the sampling frequencies lead to a situation when the receiver does resampling of the received signal by a non-integer number of original samples. This leads to the loss of the mutual orthogonality between subcarriers and, thus, ICI.

In order to determine the impact of frequency offsets in GUR-based PMC systems, a series of simulations have been made. The simulated PMC system was based on a CCRAOT transform (see 3.1.4.2) with 64 subcarriers and 16-chip padding.

Sending of just one block (80 chips) assumes a perfect timing synchronization (see Chapter 4), because without timing synchronization the impact of sampling frequency offset will be much larger. As it was mentioned in Section 4.2.3, generally, GUR-based PMC systems are very sensitive to timing offsets. Both SFO and CFO create a gradually increasing timing offset, which must be corrected.

Simulation results showed extremely high sensitivity to CFO, what emphasizes the importance of good frequency synchronization. Moreover, the impact of CFO is much larger than the impact of SFO (see the comparison in Figure 5.1 - right). This is because CFO has an immediate impact on the received TD samples, whereas the impact of SFO grows with time and, in case of good timing synchronization, the first samples always remain correct.

5.3 Carrier frequency offset estimation

In order to perform carrier frequency synchronization, it is necessary to estimate FCFO. FCFO estimation methods can be classified using several criteria. In accordance with [31] by Meyr et al., generally there are three types of estimators: DD estimators, DA estimators and NDA or blind estimators.

Since signals in MC communication systems are transformed between the TD and other domains, FCFO estimation can be performed in either TD or transform domain. FCFO estimation in the FD is widely used in OFDM-based communication system receivers. However, FCFO estimation in the GUR domain is not explored yet.

In this doctoral thesis the usability of the following FCFO estimation methods in GUR-based PMC systems is examined:

- phase of UW prefix AC result;
- phase increment of UW block XC result.

Moreover, the *average phase increment* method is reviewed as potentially useful.

5.3.1 Data-aided fractional carrier frequency offset estimators

The described TD FCFO estimators employ repeating parts of TD signal. Repeating parts are usually located at the beginning of the frames or blocks (see TD signal structure in Figure 2.4).

If we have an ideal communication channel with no dispersion and noise, then the received TD baseband signal is described by (5.1). Multiplication of two equal samples at the transmitter side $x(k) = x(k + D)$, having the temporal distance of D samples between each other, gives:

$$y(k)y^*(k + D) = |x(k)|^2 e^{j2\pi\varepsilon D} \tag{5.3}$$

FCFO can be expressed directly from (5.3) as follows:

$$\varepsilon = \frac{\angle(y(k)y^*(k + D))}{2\pi D} \tag{5.4}$$

5.3.1.1 Repeating block autocorrelation

For higher estimation accuracy, a series of multiplications can be averaged over the block with length M and it leads to an AC-based FCFO estimator. Since all phase increments are expected to be the same, the complex exponent can be brought out of the sum:

$$J = \sum_{k=0}^{M-1} y(k)y^*(k + D) = e^{-j2\pi D\varepsilon} \sum_{k=0}^{M-1} |y(k)|^2 \tag{5.5}$$

from where FCFO can be expressed as:

$$\varepsilon = \frac{1}{2\pi D}\angle\left(\sum_{k=0}^{M-1} y(k)y^*(k + D)\right) \tag{5.6}$$

This is so-called D-spaced DA FCFO estimator [31]. Since the argument of (5.6) cannot exceed π, the detection range of the mentioned estimator is limited by the condition:

$$\varepsilon_{max} = \frac{1}{2D} \tag{5.7}$$

Notice, that the detection range depends on the length of the correlation window D. To extend FCFO estimation range, two approaches can be used:

- oversampling of received chips;
- shortening of correlation window.

FCFO in a GUR-based PMC system can be estimated and corrected in the TD. Since UW is repeated at the beginning of each block, it is possible to use the pilot block AC algorithm (5.5). The diagram of the resulting FCFO estimator is shown in Figure 4.2

5.3.1.2 Maximum likelihood AC-based FCFO estimator

An ML FCFO estimator based on AC of CP was proposed by the authors of [23]. Derivation of the following ML estimator for a system using UW follows from Equation (5.5) and is obtained along with ML BTO estimator (see Section 4.2.2.1).

Maximization of the log-likelihood function with respect to FCFO leads to the following result:

$$\hat{\varepsilon}_{ML} = -\frac{1}{2\pi}\angle(\hat{\theta}_{ML}) + n, \tag{5.8}$$

where $\hat{\theta}_{ML}$ is the estimated timing offset from (4.4). The given result is suitable for systems where all received samples have Gaussian PDFs. In the meantime, many training sequences, like ZC (see Section 2.3.2.1), have other probability distributions and the described ML estimator does not fit to such systems.

5.3.2 Decision-directed fractional carrier frequency offset estimators

The proposed DD FCFO estimation algorithms are based on the XC between a known training sequence stored in the receiver and received samples. New FCFO estimators proposed in the doctoral thesis are derived from decision-directed algorithms described by Meyr et al. in [31].

If there are no any received signal impairments, except CFO, the received baseband signal is described by (5.1). Multiplication of respective transmitted and received samples yields the following result:

$$y(k)x(k)^* = |x(k)|^2 e^{j2\pi\varepsilon k} \tag{5.9}$$

From Equation (5.9) can be seen that the phase of $y(k)x(k)^*$ grows linearly in time with a speed which is proportional to the CFO. Using this observation, we can derive an XC-based FCFO estimator. Let's take two sample pairs with indexes k and $k + D$, where D is an integer offset. If multiplication of the second sample pair is described by an expression similar to (5.9):

$$y(k+D)x(k+D)^* = |x(k+D)|^2 e^{j2\pi\varepsilon(k+D)}, \tag{5.10}$$

then subtracting the arguments of Equations (5.9) and (5.10) results in:

$$\angle[y(k+D)x(k+D)^*] - \angle[y(k)x(k)^*] = 2\pi\varepsilon D \tag{5.11}$$

Now CFO can be expressed from (5.11) as follows:

$$\varepsilon = \frac{\angle[y(k+D)x(k+D)^*] - \angle[y(k)x(k)^*]}{2\pi D} \tag{5.12}$$

5.3.2.1 Method with increment averaging

Averaging the offsets within a block of adjacent samples ($D = 1$) allows to obtain an expression, which can be used in a real FCFO estimator:

$$\varepsilon = \frac{1}{2(M-1)\pi}\sum_{k=0}^{M-2}\left(\angle(y(k+1)x(k+1)^*) - \angle(y(k)x(k)^*)\right) \tag{5.13}$$

Noticeably, that the detection range of the proposed estimator is still limited by the condition (5.7). However, due to the fact that $D = 1$ in this estimator, $\varepsilon_{AVGmax} = 1/2$.

5.3.2.2 Least squares-based method

Expression (5.13) performs an averaging-based line fit within a block of samples. However, simple averaging of phase increments is not optimal in the sense of mean squared error (MSE). A least squares (LS) estimator based on a simple linear regression [32] minimizes MSE and improves the performance of the device. Replacing the averaging with an LS estimator, after some mathematical manipulations we obtain an expression:

$$\varepsilon = \frac{1}{2\pi}\sum_{k=0}^{M-1}\frac{(\alpha(k) - \sum_{m=0}^{M-1}\alpha(m))(k-\overline{k})}{\sum_{m=0}^{M-1}(k-\overline{k})^2} \tag{5.14}$$

Since $D_{LS} = 1$, the frequency acquisition range of the proposed estimator (5.14) remains $\varepsilon_{max} = 1/2$.

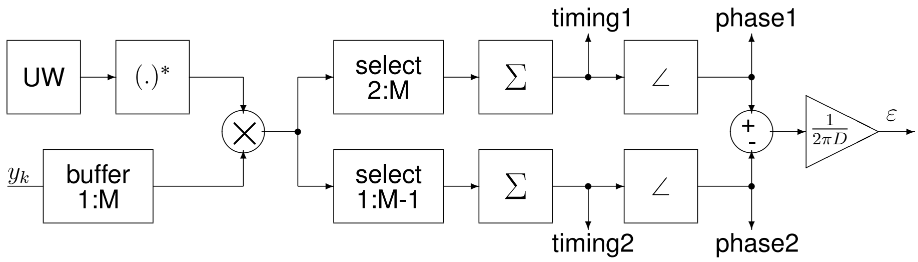

Figure 5.2: XC-based FCFO estimator optimized to use CAZAC sequences

5.3.2.3 Method for CAZAC sequences

Equation (5.13) can be changed if we use training samples from CAZAC sequences. Such training samples can be obtained, for example, using the ZC algorithm [24]. Using this method, (non-linear) complex argument operation can be exchanged with the sum. In this case Equation (5.13) can be rewritten as:

$$\varepsilon = \frac{1}{2(M-1)\pi}\left(\angle\sum_{k=0}^{M-2} y(k+1)x(k+1)^* - \angle\sum_{k=0}^{M-2} y(k)x(k)^*\right) \tag{5.15}$$

In this variant of XC-based FCFO estimator, the argument is taken from the averaged XC between the training block pattern and the received samples. The largest advantage of the estimator (5.15) is that it can be used in conjunction with the XC-based timing offset estimator described in Section 4.2.2.2. The resulting FCFO estimation scheme is shown in Figure 5.2. If sequences with good correlation properties are used in the role of UW, the magnitude of either "timing" signal can be used for BTO estimation.

5.3.2.4 Simulation results of decision-directed FCFO estimators

The accuracy of the proposed FCFO estimators has been verified using computer simulations. The transmitted sequence contained 100 blocks, each consisting of $N = 64$ random data chips and a UW with three different lengths produced using the ZC algorithm (see Section 2.3.2.1).

The purpose of the first set of the simulations was to determine the dependency of MSE on signal-to-noise ratio (SNR) at various block lengths. MSEs obtained during the simulations are depicted in Figure 5.3. The plots with legend "AC" correspond to the AC-based estimator (5.6). Abbreviations "AVG", "LS" and "CZ" correspond to the respective XC-based algorithms (5.13), (5.14) and (5.15).

From the simulation results shown on the left side of Figure 5.3 (a PMC system with an AWGN channel), it can be seen that, at small FCFO ($\varepsilon = 0.001$), the MSE of AC-based estimator is an order of magnitude smaller than those of XC-based ones. Additionally, at relatively high SNR, the accuracy of XC-based estimator (5.14) starts to surpass the accuracy of AC-based one. Among the proposed XC-based FCFO estimators, the LS-based solution (5.14) demonstrates the best results, therefore confirming the excellence of this signal processing technique.

Simulation results, shown on the right side of Figure 5.3, correspond to testing the FCFO algorithms in a PMC system with a dispersive channel having a 4-tap long impulse response. The accuracy of XC-based estimators was degraded severely, whereas the MSE of AC-based estimator remained almost unchanged. Static convolution in the communication channel affects both samples of AC-based estimator in equal manner, therefore its influence is compensated. It may be suggested, that in time-variant communication channels the AC-based estimator would perform much worse, whereas the accuracy of XC-based estimator would not change significantly.

The results of both simulations show that the accuracy of AC-based estimation is proportional to the frequency offset, whereas XC-based estimators have an almost constant MSE over the whole frequency offset range. The simulation results show also that the increase of the synchronization pattern length leads to the increase of FCFO estimator accuracy.

It must be taken into account, that sufficiently large training sequences must be used in order to achieve sufficient accuracy. For example, a 64 sample sequence provides $MSE = 10^{-8}$ at $SNR = 20dB$. However, the LS-based method described in Section 5.3.2.2 is more sensitive to additive noise and its accuracy at $SNR < 10dB$ does not increase with the increasing of UW length.

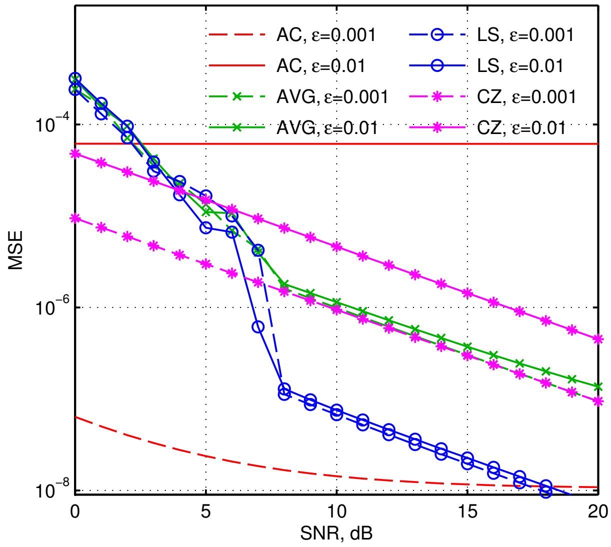

Figure 5.3: Accuracy of the FCFO estimators in a PMC system with an AWGN channel (left) and with a dispersive channel (right). The UW length is 64 samples.

5.3.3 Combined fractional carrier frequency offset estimator

AC- and XC-based FCFO estimators described in Sections 5.3.1.1 and 5.3.2, respectively, have different acquisition ranges and accuracies. An algorithm that combines these two estimators is described in the doctoral thesis, uses XC for coarse FCFO estimation, whereas for fine FCFO estimation AC is used. Using described algorithm combiner provides an efficient FCFO estimation solution with a wide acquisition range and high accuracy.

5.4 Residual phase offset estimation

As it was said before, CFO leads to a linearly increasing phase offset of the received samples. Although the previously mentioned methods are able to estimate CFO, the estimation of *residual phase* offset is necessary.

The cross-correlators used for timing estimation (see Section 4.2.2.2) and the ones used for CFO estimation (see Section 5.3.2) perform multiplication of a known reference signal and the received waveform. This operation resembles the mixing in classic phase detectors and allows to find the phase offset of the signal.

It is sufficient to take the phase of the cross-correlation result in order to obtain the phase offset. However, if an uncorrected CFO is present, a correct phase offset will be given only for the first sample, since the phase offset increases due to CFO. Therefore, the phase offset estimation unit must be directed by the timing offset estimator in order to obtain a correct phase offset. In Figure 5.2 it is shown how to obtain phase estimates (outputs 'phase1' and 'phase2') using a CAZAC sequence-based FCFO estimator.

5.5 Carrier frequency offset and phase correction

Most of the FCFO correction methods are based on the multiplication of the received signal by a complex exponent having a frequency which has opposite sign compared to the FCFO. If we have the received signal (5.1) with FCFO denoted as ε, then multiplication of this signal by FCFO compensation signal $v(k) = e^{-j2\pi\varepsilon k}$ leads to the received signal without CFO.

There are two approaches how to provide interaction between the FCFO estimator and FCFO correction devices: open-loop synchronizer and feedback (closed-loop) synchronizer. In accordance with [33], open-loop synchronizers are faster than feedback loop ones, since synchronization must be established in one step without iterations.

5.5.1 Phase offset correction

In most of the cases, for carrier phase correction, multiplication with the phase rotator $e^{-j\alpha}$ is sufficient. However, modern OFDM systems employ a Farrow variable delay filter [34], which allows to achieve better results. This is because, besides the residual phase offset, there is a fractional delay of the signal, which cannot be compensated by relatively coarse timing offset correction (see Section 4.2).

5.6 FCFO synchronizer in GUR-based PMC system

In this doctoral thesis detailed simulation results of a closed-loop synchronizer in a GUR-based PMC system are provided. A complex exponent signal for FCFO compensation was produced by NCO. NCO, in turn, was controlled by PID controller, whose input signal was FCFO measured by the estimator. FCFO synchronization was simulated in two modes: acquisition mode and tracking mode. The simulated feedback FCFO synchronizer provided stable synchronization in FCFO range $-0.01 < \varepsilon < +0.01$.

Conclusions

- In order to provide a BER less than 10^{-3} in a CCRAOT-based MC communication system with 64 subcarriers, FCFO must be less than 0.001, i.e. 1000 ppm.
- AC-based FCFO estimator provides high-accuracy estimates, but its estimation range is strongly limited.
- UW XC-based FCFO estimator provides a suitable estimation range at a moderate estimation accuracy. However, in communication systems with frequency-selective channels, the accuracy of XC-based CFO estimator is insufficient.
- Combination of AC-based and XC-based FCFO estimators can provide a sufficient FCFO estimation accuracy and a wide estimation range.
- Simulated feedback FCFO synchronizer provides stable synchronization in FCFO range -0.01–0.01.

6 Channel estimation and equalization

This chapter is aimed to solve the problem of equalization in GUR-based PMC systems. The ultimate goal is to develop a GD equalizer.

6.1 Introduction

In a real communication system, due to dispersion, reflection and multipath propagation in the communication channel, several distorted and shifted copies of the same signal are received. Moreover, the impact of channel can vary in time. There are two approaches for providing a correct demodulation of signals transmitted over dispersive media:

- It is possible to use *differential modulation* , for instance, differential quadrature amplitude modulation (DQAM) or differential phase shift keying (DPSK), and measure relative variations of the adjacent samples. This technique makes it possible to transmit information without the equalization, but at the same time, results in a reduced capacity of the communication channel.
- The second approach is to use *coherent detection* . In such a case, the information on the current impact of the communication channel on subcarriers can be obtained through the channel estimation (see Section 6.4). Channel estimates, in turn, can be used for reversing the changes inferred by the communication channel, i.e. equalization (see Section 6.5).

6.2 System model

In a PMC system where the transmitter baseband TD output signal $x(t)$ is being transferred via the baseband equivalent of the communication channel with the impulse response $h(t)$, the receiver input signal $y(t)$ can be described as follows:

$$y(t) = x(t) * h(t) + w(t), \tag{6.1}$$

where $w(t)$ is additive noise. If a transmitted signal is sampled with the sample time T_s and grouped into blocks (vectors) $\boldsymbol{x}$, and there is no IBI, then communication can be described by Equation (2.5). In order to recover the transmitted information, the receiver must reverse the changes inferred by the communication channel by means of an equalizer:

$$\boldsymbol{x} = \boldsymbol{H}^{-1}(\boldsymbol{y} - \boldsymbol{w}) \tag{6.2}$$

However, the inversion of Toeplitz matrix $\boldsymbol{H}$ in equation (2.5) can not performed easily. Moreover, this matrix must be acquired by the receiver using means of *channel estimation* (see Section 6.5) of the channel impulse response samples h_i must be performed before equalization.

In an MC communication system, each sample of the information vector actually is the spectrum coefficient for some basis function of the transform $\boldsymbol{\Phi}$. Therefore, TD samples $\boldsymbol{x} = \boldsymbol{\Phi}^{-1}\boldsymbol{X}$ are obtained using the inverse transform. Then (2.5) can be rewritten as follows:

$$\boldsymbol{y} = \boldsymbol{H}\boldsymbol{\Phi}^{-1}\boldsymbol{X} + \boldsymbol{w}, \tag{6.3}$$

where $\boldsymbol{X}$ is the transform domain input vector, $\boldsymbol{\Phi}^{-1}$ is the inverse of the unitary transform matrix. The received vector is transformed back into the transform domain, equalized and passed to the QAM detector. The receiver operation can be described as follows:

$$\hat{\boldsymbol{X}} = \boldsymbol{A}^{-1}\boldsymbol{\Phi}\boldsymbol{y}, \tag{6.4}$$

where $\boldsymbol{A}^{-1}$ is the equalizer matrix, which can be obtained by inverting the transform domain channel matrix $\boldsymbol{A}$:

$$\boldsymbol{A} = \boldsymbol{\Phi}\boldsymbol{H}\boldsymbol{\Phi}^{-1} \tag{6.5}$$

6.3 Disturbances caused by the communication channel

Due to various effects in the communication channel as well as in the transmit (see Section 2.4) and receive filters, there is mutual interference between the received samples. In MC communication systems, this interference is divided into two types:

- Disturbance from the other symbols - ISI;
- Disturbance from the other subcarriers - ICI.

6.3.1 Inter-symbol interference

In order to avoid ISI, the first Nyquist criterion [35] must be fulfilled:

$$h^{\mu\mu}(k) = \delta(k)\begin{cases} 1 & \text{if } k = 0 \\ 0 & \text{if } k \neq 0 \end{cases} \quad \text{where} \quad h^{\mu\mu}(k) = \varphi_t(\mu, k) * h(k) * \varphi_r(\mu, k) \tag{6.6}$$

where $\varphi_t(\mu, k)$ is the transmitter BF at the subcarrier $n = \mu$ and $h(k)$ is the channel impulse response, and $\varphi_r(\mu, k)$ is the receiver BF at the subcarrier $n = \mu$. If this condition is fulfilled, there is no interference between subsequent *transform domain* samples on a certain subcarrier.

6.3.2 Inter-carrier interference

ICI $h^{\mu\eta}(t)$ shows the amount of interference between the subcarriers:

$$h^{\mu\eta}(k) = 0 \quad \forall k \quad \text{where} \quad h^{\mu\eta}(k) = \varphi_t(\mu, k) * h(k) * \varphi_r(\eta, k) \tag{6.7}$$

If this condition is fulfilled, there is no interference between *transform domain* samples belonging to the same block.

6.3.3 Double orthogonality condition

If zero interference conditions (6.6) **and** (6.7) **are hold, it said that *double orthogonality condition* is fulfilled.** In this case the transform domain channel matrix $\boldsymbol{A}$ in Equation (6.5) becomes diagonal.

6.4 Channel estimation

In order to provide equalization, information about the communication channel characteristics, i.e. CSI is necessary. If characteristics of the communications channel do not vary, one can measure it beforehand and then assume that CSI is known. Otherwise, dynamic measurement of CSI, i.e. channel estimation is necessary.

Channel estimation can be performed by analyzing the properties of the received signal. In this case it is said that *blind* channel estimation and equalization are performed. On the other hand, the method of channel estimation using special training signals is widely used. In this case it is said that *pilot signal assisted modulation (PSAM)* is used, and the channel is estimated by comparing received training sequences with transmitted ones.

6.4.1 Time domain channel estimation

There is a big variety of TD channel estimation methods, which have been developed since 1860 [36]. Since in GUR-based PMC system signal processing at the receiver side starts in TD, most of TD channel estimation and equalization methods are suitable to GUR-based PMC systems. On other hand, it must be noticed, since the TD is a specific case of the more general GD, all GD channel estimation methods must work in the TD, too. The doctoral thesis describes several TD channel estimation methods, however, only the two most important ones will be mentioned here.

6.4.1.1 Back-substitution method

The rhombus-like structure of the *convolution matrix* allows to use *back-substitution* in order to provide channel estimation. It is similar to solving a system of linear equations using the Gauss-Seidel method (method of successive displacement) [37]. A drawback of the given method is that it accumulates the error, caused by the unknown noise component w, which is present in the received vector. Therefore, the last samples of the channel impulse response $\boldsymbol{h}$, which are obtained in the last iterations, are most imprecise.

6.4.1.2 LMS system identification method

The channel impulse response can be obtained by means of adaptive least mean squares (LMS) filter [38] in system identification mode. Unlike equalization mode (see Section 6.5.1), the filter takes the actual receiver input as a target and training blocks as (non-equalized) input. In other words, system identification mode can be obtained by just swapping inputs of LMS filter in equalization mode. In accordance with simulations described in Section 6.6, LMS system identification can provide means for very accurate channel estimation.

6.4.2 GUR domain channel estimation

GUR can produce a wide variety of transforms, including well-known ones, such as DFT, Identity transform and others (see Section 3.1). *For PMC systems (see Section 3.4.1) a flexible GD channel estimation method, which is usable in all possible domains, is required.*

6.4.2.1 Identity matrix method for GD channel estimation

Using this method, a channel estimate can be obtained by transmitting an identity matrix-based training sequence. In this case, an estimate of the channel matrix $\hat{\boldsymbol{A}}$ appears at the output of unitary transform in the receiver each time when the training sequence is transmitted. However, this kind of channel estimation is far from optimal, since the training sequence is long and has many zeros and, therefore, it is susceptible to the noise.

6.4.2.2 GD channel estimation using conversion from the TD

Another way, how to obtain the GD channel estimate $\hat{\boldsymbol{A}}$, is to calculate it from the TD channel estimate (see Section 6.4.1) using (6.5). In this case, all classical TD channel estimation methods are applicable.

6.4.3 Frequency domain channel estimation

FD channel estimation is widely used in OFDM communication systems due to low computational complexity and high efficiency in systems with slowly changing frequency-selective, i.e. time-dispersive channels. A necessary condition for FD equalization is fulfillment of the double orthogonality condition (see section 6.3.3). FD estimation is based on transmission of training subcarriers called *pilot tones*.

The doctoral thesis contains a detailed description of the FD channel estimation algorithm. Unfortunately FD channel estimation cannot be used in PMC systems, which employ basic (see table 3.1) GUR transforms, because convolution in the communication channel and filters causes ICI, which forbids the use of the aforementioned algorithm. However, in the future (see Chapter 8) it is planned to develop such parametric unitary transforms, which do not cause transform domain ICI. In this case FD channel estimation and FDE methods will be usable in PMC systems.

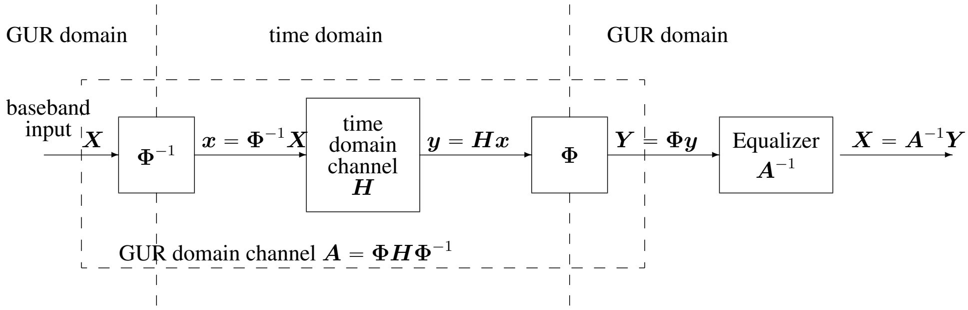

Figure 6.1: GD channel equalization problem

6.5 Channel equalization

6.5.1 Time domain equalization

TD equalization is based on the classic adaptive algorithms, such as LMS and recursive least squares (RLS). These algorithms iteratively adjust the coefficients of the FIR filter in order to minimize the difference between the desired signal and the filter output. More details about these algorithms can be found in the book [38], written by one of the inventors of the LMS algorithm. TD equalization can be used both with inserted and super-imposed (see Section 2.3.1) training signals.

As it was mentioned before, TD equalization can be successfully used in parametric GUR-based PMC systems.

6.5.2 Frequency domain equalization

If the TD channel matrix $\boldsymbol{H}$ is a *circulant* matrix [39], then the transform domain channel matrix $\boldsymbol{A}$ is *diagonal*, because from (6.5) follows the *eigendecomposition* of the channel matrix $\boldsymbol{H}$:

$$\boldsymbol{A} = \boldsymbol{F}\boldsymbol{H}\boldsymbol{F}^{-1} \tag{6.8}$$

In turn, the matrix $\boldsymbol{H}$ becomes circulant, if blocks with CP (see Section 2.2.4.1) are used, which leads to the circular convolution between the transmitted TD samples $\boldsymbol{x}$ and the channel impulse response $\boldsymbol{h}$. Therefore, the combination of CP and DFT leads to the fulfillment of the *double orthogonality* condition.

The doctoral thesis contains a detailed description of FDE. Unfortunately the FDE technique is not compatible with PMC systems, who employ ordinary (see table 3.1) GUR transforms. However, as it was already mentioned in Section 6.4.3, if PMC system, where transform domain ICI is eliminated, will be developed, it will use FDE.

6.5.3 GUR domain equalization

If condition (6.7) is not fulfilled, transform domain channel matrix $\boldsymbol{A}$ is *not diagonal* anymore, thus double orthogonality condition (see Section 6.3.2) is not fulfilled. The inversion of non-diagonal GD channel matrix $\boldsymbol{A}$ requires an additional effort. The problem of GD equalization is explained in Figure 6.1.

6.5.3.1 SVD-based equalization

One of the great methods to perform a pseudo-inversion of a non-square matrix is the singular value decomposition (SVD) [40]. SVD decomposes a given rectangular matrix into two unitary square matrices $\boldsymbol{U}$ and $\boldsymbol{V}$, which share common eigenvalues, and a diagonal matrix $\boldsymbol{S}$ with singular values sorted in descending order:

$$\text{if} \quad \boldsymbol{A} = \boldsymbol{U}\boldsymbol{S}\boldsymbol{V}^{-1} \quad \text{then} \quad \boldsymbol{A}^{-1} = \boldsymbol{V}\tilde{\boldsymbol{S}}\boldsymbol{U}^{-1} \tag{6.9}$$

The pseudo-inverse of this non-square $\boldsymbol{A}$ now can be found easily, since for unitary matrices $\boldsymbol{V}^{-1} = \boldsymbol{V}^{*}$. The elements of the inverted diagonal rectangular matrix contain reciprocal values of the original matrix $\tilde{S}_{kk} = 1/S_{kk}$, where $k \in [1, K]$.

SVD-based equalization is a known method, considered, for example, in [41]. However, due to large computational complexity it is not popular. Still, SVD is a perfect choice for the PMC systems, because this equalization will continue to work after the change of unitary transformation.

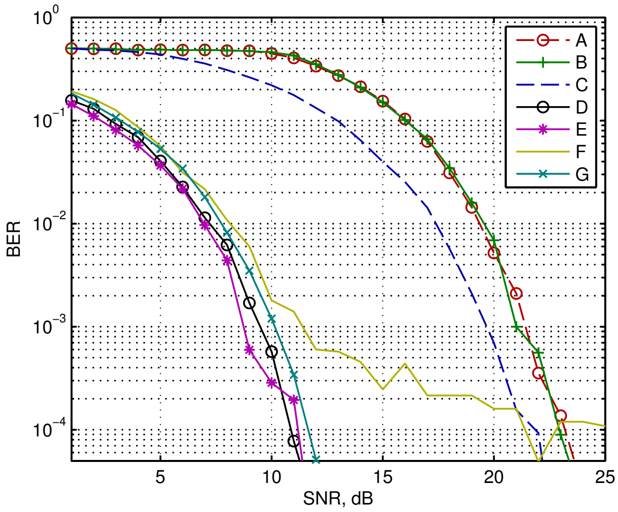

Label	Estimation method	Equalization method
A	TD-identity matrix	GD-SVD
B	GD-identity matrix	GD-SVD
C	TD-δ	GD-SVD
D	TD-LMS	GD-SVD
E	ideal (known channel)	GD-SVD
F	TD-LMS	TD-LMS
G	FD	FD

Figure 6.2: Performance comparison of various estimators and equalizers

6.6 Simulation results of equalization

A baseband PMC system with perfect timing and frequency synchronization was built for the simulations. CCRAOT with $\phi = \frac{\pi}{6}$, $\psi = 0$, $\gamma = \frac{\pi}{2}$ was used in the role of GUR transform $\mathbf{\Phi}$. Transmission was carried out in frames consisting of 64 training blocks and 20 payload blocks. ZP blocks consisting of 64 payload samples and 16 padding samples were used in all simulations. Adaptive LMS filters for both equalization and system identification (estimation) were 8 taps long. Seven different PMC systems were simulated and compared. The simulation results in the form of BER plots of PMC systems are depicted in Figure 6.2.

From Figure 6.2 can be concluded, that SVD provides an efficient method for GD equalization in a PMC system. The highest PMC system performance can be achieved using an LMS-based TD channel estimator in conjunction with an SVD-based GD equalizer. **This equalizer has better performance than an FD estimator with FDE i.e. OFDM, using the same number of training samples**.

6.7 Comparison of channel estimation and equalization methods

The goal of this section is to describe the results of an experiment [15], where different combinations of unitary transforms and equalizers were tried. The objective of those simulations was to examine the following questions:

- Impact of the choice of unitary transform on BER of MC system;
- Impact of transform on the efficiency of equalization;
- Impact of equalization method on BER of MC system;
- Compatibility between unitary transforms and equalization methods;
- Impact of PAPR of the TD signal on BER of MC system having a nonlinear channel.

The results of these simulations are given in the doctoral thesis. At the beginning of writing the doctoral thesis, they allowed to understand better the nature of the channel impact in various transformation domains. Useful conclusions about the applicability of different equalization methods to different MC systems are made.

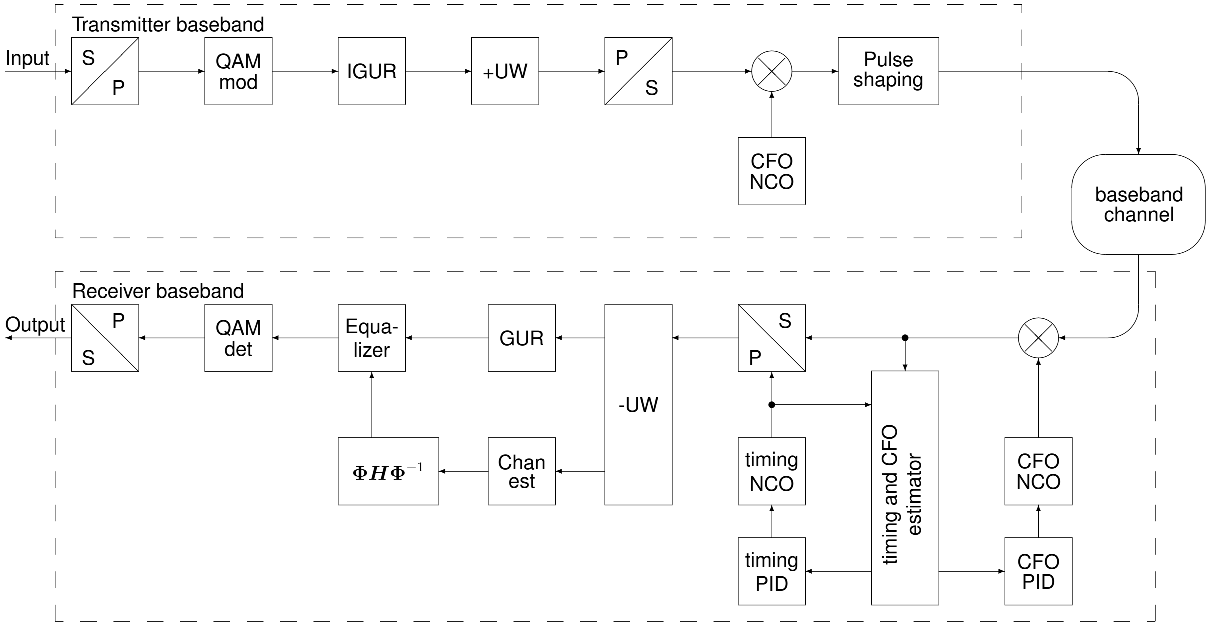

Figure 7.1: Block diagram of the modeled PMC system

Conclusions

- In a PMC system with an AWGN channel the performance of all transforms is the same.
- LMS is applicable to TD equalization only.
- FD channel estimation and equalization techniques are not applicable to CCRAOT domain.
- SVD provides a precise method for GD equalization.
- SVD-based equalizer can be used in PMC systems with a variable transform.
- Highest PMC system performance can be achieved using an LMS-based TD channel estimator in conjunction with an SVD-based GD equalizer.

7 Design of parametric multicarrier modulation system

The purpose of the given chapter is to prove the viability of the proposed synchronization and equalization methods and verify their mutual consistency.

This chapter describes a complete example of one particular GUR-based PMC system baseband, using a selection of the previously described methods. Although proven methods are selected to obtain maximum performance (in terms of BER) of the PMC system, the proposed design can be considered as initial implementation. All elements of the PMC system are based on the solutions presented in the previous chapters.

7.1 Structure of the parametric multicarrier modulation system

The physical layer of a PMC system is described in detail in Section 2.1. The particular PMC system described in this chapter follows the structure depicted in Figure 2.1. However, this PMC system does not include an RF parts and channel encoder/decoder. The structure of the described *baseband* PMC system is depicted in Figure 7.1. A baseband signal from the transmitter baseband propagates via the baseband equivalent of RF communication channel and after that enters the baseband of the PMC system receiver.

7.1.1 Transmitter

Detailed transmitter operation is described in Section 2.1.1. The most important operation within the transmitter – GUR-based MC modulator (see details in Section 3.1) is based on the most basic structure of the

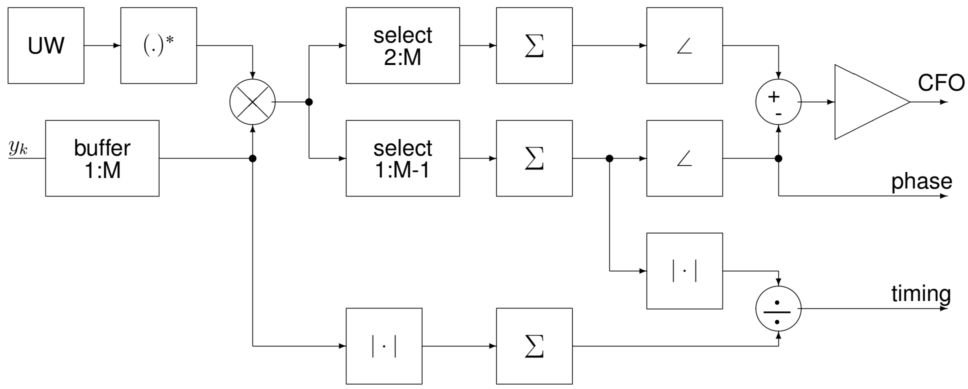

Figure 7.2: XC-based BTO and CFO estimator

unitary transform unit – matrix type transform unit (see Section 3.2.1). The test configuration is based on a 64-dimensional CCRAOT (see Section 3.1.4.2), which is the most basic type of GUR.

For timing and frequency synchronization as well as for channel estimation the UW padding (see Section 2.2.4.3) is used. ZC sequences (see Section 2.3.2.1) are selected as the most appropriate type of UW sequences in terms of correlation and envelope properties. For investigation of the impact of CFO, an appropriate local oscillator (unit 'CFO NCO') is added to the transmitter. Before output to the communication channel, 4x upsampling and pulse shaping (see Section 2.4), based on a classic root-raised-cosine (RRC) FIR filter with 65 coefficients, are performed.

7.1.2 Receiver

The receiver of the modeled PMC system incorporates a timing synchronization circuitry (see Chapter 4), frequency synchronization units (see Chapter 5), a GUR-based MC demodulator (see Chapter 3) and an equalizer (see Chapter 6). The structure of the proposed receiver corresponds to the general structure proposed in Section 2.1.2.

7.1.2.1 Timing and frequency synchronization

All timing and frequency offset estimation is performed by processing of the received UW prefixes, generated at the transmitter. A UW prefix is added to each data block and is 16 samples long. Timing and CFO estimation is performed by means of a combined estimator, shown in Figure 7.3. It consists of AC and XC estimators.

The estimator, shown in Figure 4.2 is based on AC . For block timing estimation it uses the algorithm described in Section 4.2.2.1, whereas for CFO estimation the algorithm from Section 5.3.1.1.

Another estimator, shown in Figure 7.2, is based on the XC of the received samples with the UW pattern stored in the receiver. The operation of timing estimator is described in detail in Section 4.2.2.2, whereas CFO estimation is performed by means of the algorithm described in Section 5.3.2. Besides timing and CFO estimation, the combined XC estimator performs residual phase offset estimation (see Section 5.4).

The combining of estimator results is performed by the unit shown in Figure 7.3. This unit incorporates both previously mentioned estimators and contains the logic for switching between them. The block timing estimate combiner used here is based on the algorithm described in Section 4.2.3, and the CFO estimate combiner employs the algorithm described in Section 5.3.3.

For BTO correction a *feedback* or *closed-loop* synchronizer (see Section 4.2.3) is used. The value of the estimated timing offset enters the timing PID controller ('timing PID' in Figure 7.1), which is necessary to generate the driving signal for the timing NCO and to stabilize the automatic control loop, responsible for the timing.

CFO is corrected using another feedback-type synchronizer. For CFO compensation, multiplication with a complex exponent signal, having a frequency opposite to CFO, is used (see Section 5.5). For this purpose, the estimated values of CFO and phase offset are passed from the combined timing and CFO estimator to the CFO PID controller. This controller generates a signal that drives NCO, responsible for CFO compensation.

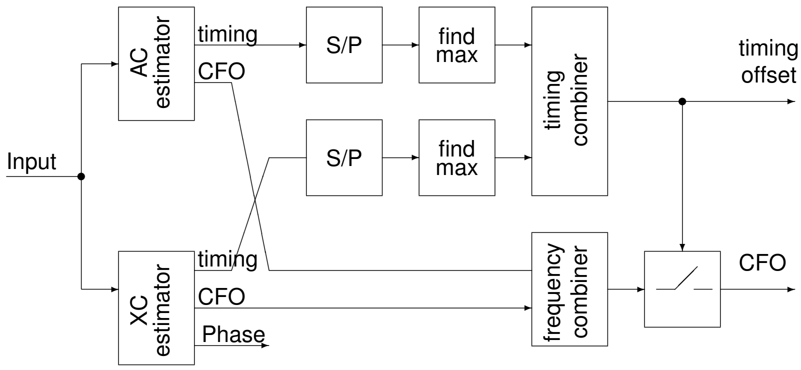

Figure 7.3: Combined timing and CFO estimator

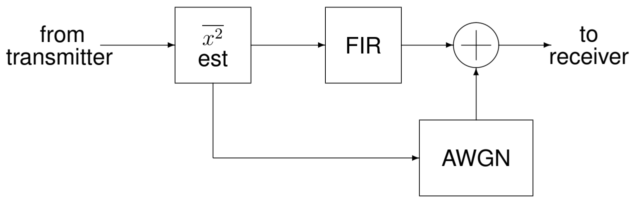

Figure 7.4: Communication channel model (the “baseband channel” unit)

7.1.2.2 Channel estimation and equalization

In model of a PMC system a TD estimator, based on an LMS filter in system identification mode (see Section 6.4.1.2), is used. According to the simulation results from Section 6.6, LMS provides the most accurate estimate of the communication channel. The number of coefficients of the LMS estimator must be larger than the length of channel impulse response (a model uses 8 coefficients).

The model of the PMC system contains an SVD-based equalizer (see Section 6.5.3.1), since this is currently the only method that provides equalization in the GD.

7.1.3 Baseband communication channel

Since the given doctoral thesis is one of the first attempts to describe synchronization and estimation algorithms for GUR-based PMC systems, the work is limited to the basic channel model including two major effects: time-dispersion (frequency-selectivity) and additive noise. Moreover, since RF part is not included into the model, a *baseband equivalent* communication channel is modeled. This baseband equivalent channel is obtained by “downconversion” of passband channel properties into baseband. Since only the basic properties of communication channel – dispersion and noise are modeled, this conversion is straightforward.

The model of GUR-based PMC system has been built using a communication channel model containing the superposition of FIR filter and AWGN source. The structure of the communication channel model is shown in Figure 7.4. The additional unit ‘$\overline{x^2}$ est’, which appears in Figure 7.4, is necessary for signal power estimation, which is used for adjusting the AWGN power, in order to achieve required SNR.

7.2 Simulation results of the model

The performance of the created PMC system model has been tested with various channel parameters. SNR of the receiver input signal has been changed in a range from 0 dB to 30 dB. The length of channel impulse response has been varied from 1 tap to 15 taps. Since the transmitter and receiver use 4x oversampling of the TD signal in order to provide pulse shaping and timing synchronization, an efficient length of channel impulse response is smaller (in Figure 7.5 shown in brackets) than the order of the FIR filter of the channel model.

The performance of the PMC system at various lengths of communication channel impulse response is shown in Figure 7.5. It is seen that the increase of the length of channel impulse response leads to the degradation of PMC system throughput. This is caused by several factors:

- LMS estimation of a channel with a longer impulse response is less precise;
- UW cross-correlation peaks get ‘washed’ by the convolution in the communication channel, and therefore, leads to increased BTO (see Section 4.2.2.2);

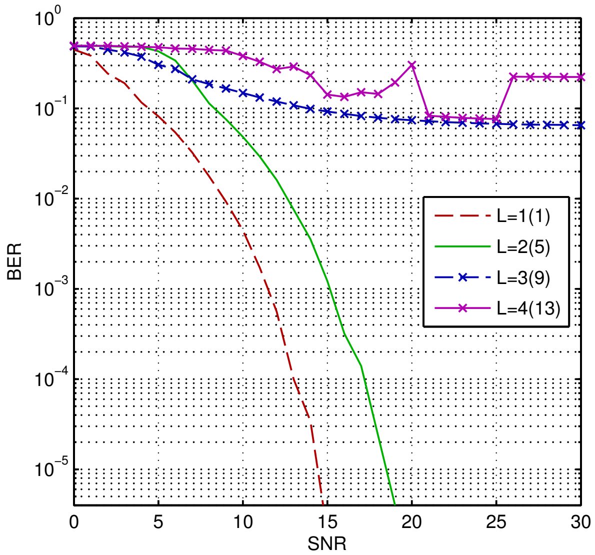

Parameter	Value
Number of subcarriers, N	64
UW length, L	16
Type of transformation	CCRAOT
CCRAOT angle ϕ	30°
CCRAOT angle γ	$\pi/2$
CCRAOT angle ψ	0
UW sequence, $\boldsymbol{u}$	ZC, $M = 3, Q = 16$
LMS length in chan. est.	8 taps
Absolute CFO, ϵ	0

Figure 7.5: Parameters and performance of the PMC system at different lengths of impulse response of the communication channel

- Phase distortions of UW sequences, caused by the convolution in the communication channel, increase the error of cross-correlation-based CFO estimator (see Section 5.3.2).

Computational complexity of the most resources-consuming algorithms is summarized in Table 7.1.

Algorithm	Complexity
Combined BTO and CFO estimator	18432
Unitary transformation	12288
Equalizer	786432

Table 7.1: Computational complexity of the algorithms

Conclusions

- GUR can be successfully used for building of PMC systems.
- ZC sequence-based UWs, that are inserted at the beginning of useful sample blocks, are reusable for simultaneous timing synchronization, frequency synchronization and channel estimation.
- Simulations have demonstrated that the proposed design of the PMC system is sufficiently stable to be used as a reference for hardware prototype.
- Complexity of the proposed solution is suitable for the implementation into software-defined radio (SDR) platform based on general purpose central processing unit (CPU) or field-programmable gate array (FPGA) chip.

8 Utilization of the obtained results for future research

This chapter aims to give the reader an overview of the research directions that the author considers are important after completing this doctoral work.

Shift-invariant GUR-based transforms

A CCRAOT-based PMC system is extremely sensitive to timing offset (see Section 4.2.1). Since a shift of the input vector by one sample causes cardinal changes in spectrum coefficients, a GUR-based PMC system requires block timing error tolerance less than one chip. The development of GUR-based *shift-invariant* transforms [42], [43] would allow to create robust PMC systems.

Inter-carrier interference free transmission

In research [9] it is shown, that *eigenfunctions* of the communication channel depend on its stationarity. Transmission using eigenfunctions would allow to eliminate ICI in PMC systems with doubly-selective channels and use low-complexity FD-like channel estimation and equalization schemes (see Section 6.5.2). Since SVD can be employed for searching the eigenfunctions, a work on GUR-based SVD algorithm is necessary. Excellent analysis and useful guidelines for the SVD-based equalization in systems with doubly-selective channels can be found in [44].

Multiple-input multiple-output

Due to the fact that unitary transforms and SVD is widely used in multiple-input multiple-output (MIMO) systems [45], a GUR-based MIMO precoder would pave a way to new possibilities. Use of GUR-based MC modulation [46] in such systems would increase their flexibility even more.

References

[1] Weinstein S. and Ebert P. Data Transmission by Frequency-Division Multiplexing Using the Discrete Fourier Transform. //Communication Technology, IEEE Transactions on. 1971. vol. 19, no. 5, pp. 628–634.

[2] Bingham J.A.C. Multicarrier modulation for data transmission: an idea whose time has come. //IEEE Communications Magazine. 1990. vol. 28, no. 5, pp. 5–14.

[3] Lindsey A. and Dill J. Wavelet packet modulation: a generalized method for orthogonally multiplexed communications. //Proceedings of the Twenty-Seventh Southeastern Symposium on System Theory. 1995, pp. 392–396.

[4] Farhang-Boroujeny B. OFDM Versus Filter Bank Multicarrier. //Signal Processing Magazine, IEEE. 2011. vol. 28, no. 3, pp. 92–112.

[5] Mattera D. and Tanda M. Data-aided synchronization for OFDM/OQAM systems. //Signal Processing. 2012. vol. 92, no. 9, pp. 2284–2292.

[6] Lopez-Salcedo J.A., Gutierrez E., Seco-Granados G., and Swindlehurst A.L. Unified Framework for the Synchronization of Flexible Multicarrier Communication Signals. //Signal Processing, IEEE Transactions on. 2013. vol. 61, no. 4, pp. 828–842.

[7] Misans P. and Torkelson M. Preliminary Simulation of Multicarrier Modulation Data Transmission System. // Nordic MATLAB Conference. Stockholm, p. 4.

[8] Tsai S.H.S. Multicode transmission using Walsh Hadamard transform. 2011.

[9] Kozek W. Matched Weyl-Heisenberg expansions of nonstationary environments. Ph.D. thesis, Vienna University of Technology. 1997.

[10] Martone M. A multicarrier system based on the fractional Fourier transform for time-frequency-selective channels. //Communications, IEEE Transactions on. 2001. vol. 49, no. 6, pp. 1011–1020.

[11] Oka I. and Fossorier M. A General Orthogonal Modulation Model for Soft-ware Rados. //IEEE Transactions on Communications. 2006. vol. 54, no. 1, pp. 7–12.

[12] Misans P. and Valters G. Initial FPGA design for generalized Orthogonal Nonsinusoidal Division Multiplexing. //2009 Norchip. 2009, pp. 1–5.

[13] Forouzan A.R. and Garth L. Orthogonal Code Design for Spectrally Encoded CDMA Systems. // GLOBECOM'07. pp. 4434–4439.

[14] Misans P., Terauds M., Aboltins A., and Valters G. MATLAB/SIMULINK Implementation of Phi-Transforms–A New Toolbox Only or the Rival of Wavelet Toolbox for the Next Decade? // Nordic MATLAB User Conference. pp. 1–8.

[15] Aboltins A. Comparison of Orthogonal Transforms for OFDM Communication System. //Electronics and Electrical Engineering. 2011. vol. 111, no. 5, pp. 77–80.

[16] Aboltins A. and Misans P. Singular Value Decomposition Based Phi Domain Equalization For Multi-Carrier Communication System. //Electronics and Electrical Engineering. 2012. vol. 18, no. 9, pp. 71–74.

[17] Aboltins A. Block synchronization using unique word for Generalized Unitary rotation based communication system. // Baltic Electronics Conference - BEC2012. Tallinn, pp. 71–74.

[18] Aboltins A. Carrier Frequency Offset Estimator Based on Unique Word Cross-correlation. // 20th Telecommunications Forum - TELFOR2012. Belgrade, pp. 486–489.

[19] Aboltins A. and Misans P. Removal of Super-Imposed Synchronization Sequence Using Matched Filter. // Microwave and Radio Electronics Week, MAREW2013. Pardubice, pp. 86–90.

[20] Misans P., Valters G., Terauds M., and Aboltins A. Initial Implementation of Generalized Haar-Like Orthonormal Transforms into FPGA-Based Devices-Part I: Signal Spectrum Analyzer-Synthesizer Module. //TELECOMMUNICATIONS AND ELECTRONICS. 2008. vol. 8, pp. 16–21.

[21] Aboltins A. and Klavins D. Synchronization and correction of channel parameters for an OFDM-based communication system. //Automatic Control and Computer Sciences. 2010. vol. 44, no. 3, pp. 160–170.

[22] Peled A. and Ruiz A. Frequency domain data transmission using reduced computationally complexity algorithms. // Acoustics, Speech, and Signal Processing, IEEE International Conference on ICASSP'80. IEEE, vol. 5, pp. 964–967.

[23] van de Beek J.J., Sandell M., and Borjesson P.O. ML estimation of time and frequency offset in OFDM systems. //IEEE Transactions on Signal Processing. 1997. vol. 45, no. 7, pp. 1800–1805.

[24] Chu. Polyphase codes with good periodic correlation properties. //IEEE Transactions on Information Theory. 1972. , no. 6, pp. 531–532.

[25] Schmidl T. and Cox D. Robust frequency and timing synchronization for OFDM. //IEEE Transactions on Communications. 1997. vol. 45, no. 12, pp. 1613–1621.

[26] Rahardja S. and Falkowski B. Family of unified complex Hadamard transforms. //Circuits and Systems II: Analog and Digital Signal Processing, IEEE Transactions on. 1999. vol. 46, no. 8, pp. 1094–1100.

[27] Valters G. and Misans P. FPGA implementation of Elementary Generalized Unitary Rotation. //2009 Norchip. 2009. , no. 2, pp. 1–4.

[28] Misans P. and Terauds M. Introduction into the fast orthogonal transforms based on rotation angles: A New Methodical approach only or a gateway to novel DSP algorithms? // ECS. Bratislava, pp. 85–94.

[29] Dita P. Factorization of Unitary Matrices. //Journal de Physique (main title). 2001. vol. A 36, p. 12.

[30] Love D.J., Heath R.W., Lau V.K.N., Gesbert D., Rao B.D., and Andrews M. An overview of limited feedback in wireless communication systems. 2008.

[31] Meyr H., Moeneclaey M., and Fechtel S.A. Digital Communication Receivers: Synchronization, Channel Estimation, and Signal Processing. Wiley series in telecommunications and signal processing. Wiley. 1998.

[32] de Sa J.P.M. Linear regression. // Applied Statistics Using SPSS, STATISTICA, MATLAB and R, chap. 6. 2007. pp. 272–285.

[33] Classen F., Meyr H., and Sehier P. Maximum likelihood open loop carrier synchronizer for digital radio. // Communications, 1993. ICC 93. Geneva. Technical Program, Conference Record, IEEE International Conference on. vol. 1, pp. 493–497 vol.1.

[34] Farrow C. A continuously variable digital delay element. // Circuits and Systems, 1988., IEEE International Symposium on. IEEE, pp. 2641–2645.

[35] Proakis J.G. Digital communications. McGraw-Hill, 4th ed. 2000.

[36] Falconer D. History of equalization 1860-1980. //Communications Magazine, IEEE. 2011. vol. 49, no. 10, pp. 42–50.

[37] Dukkipati R.V. MATLAB An introduction with applications. New Age International, New Delhi. 2010.

[38] Widrow B. and Stearns S.D. Adaptive signal processing. Prentice-Hall signal processing series. Prentice-Hall. 1985.

[39] Gray R.M. Toeplitz and Circulant Matrices: A Review. //Foundations and Trends® in Communications and Information Theory. 2005. vol. 2, no. 3, pp. 155–239.

[40] Golub and VanLoan. Matrix computations. The Johns Hopkins University Press, 3 ed. 1996.

[41] Bianchi T. and Argenti F. SVD-based equalization for zero padded multicarrier systems in time-variant fading channels. //Signal Processing. 2006. vol. 0, no. Eusipco, pp. 0–4.

[42] Yu R. Shift-Variance Analysis of Generalized Sampling Processes. //Signal Processing, IEEE Transactions on. 2012. vol. 60, no. 6, pp. 2840–2850.

[43] Almeida L. The fractional Fourier transform and time-frequency representations. //IEEE Transactions on Signal Processing. 1994. vol. 42, no. 11, pp. 3084–3091.

[44] Marzetta T.L. and Salz J. Singular Value Decomposition of a Matrix-Valued Impulse Response. //Proceedings. (ICASSP '05). IEEE International Conference on Acoustics, Speech, and Signal Processing, 2005. 2005, pp. 913–916.

[45] Raleigh G.C. and Cioffi J.M. Spatio-temporal coding for wireless communication. 1998.

[46] Park J., Chun J., and Jeong B.J. Efficient Multi-user MIMO Precoding based on GSVD and Vector Perturbation. //Signal Processing. 2011.